# Appendix O.7

# Preliminary Battery Energy Storage System Plume Study

# Starlight
# Plume Study

**DRAFT VERSION. SUBJECT TO CHANGE DUE TO REVIEW.**

HD-26 009-Starlight-Plume-0.1

April 21, 2026

*Prepared for:*

**Starlight Solar**


*By:*

**Anne Marie Hawkins**
**Anna Jensen**
**Kevin Marr, Ph.D. P.E.**
**Erik Archibald, Ph.D. P.E.**

Hazard Dynamics LLC
5555 N. Lamar Blvd, Suite J123
Austin, TX 78751 USA

# Contents

# 1 Executive Summary

A plume study was conducted for the Starlight BESS (battery energy storage system) site to determine toxicity hazards posed to nearby areas during possible battery failure scenarios. The study considers toxic species that can be released by Li-ion batteries during thermal failures. Computational fluid dynamics (CFD) models were utilized to simulate plumes resulting from theoretical battery failure scenarios. The following scenarios are considered (1) a non-fire scenario in which battery vent gas is released, (2) a small fire scenario, and (3) a large fire scenario. The fire scenarios considered low and high wind conditions based on nearby meteorological data. Atmospheric stability classes D, E, and F were modeled to evaluate a range of dispersion conditions from neutral to stable environments.

Based on the modeled scenarios, toxic gas species concentrations 2 m (6.6 ft) and 5 m (16.4 ft) from ground level were estimated using Fire Dynamics Simulator (FDS), which is a CFD software developed by the National Institute of Standards and Technology (NIST) for fire modeling. A summary of the findings of the study is as follows:

- For the vast majority of the downwind region, the fire scenarios with high wind conditions resulted in the highest modeled battery plume concentrations at 2 m (6.6 ft) from ground level. However, at approximately 200 ft from the burning BESS enclosure, the concentrations near ground level were slightly higher for some low wind conditions.
- The modeled average carbon monoxide concentrations at 2 m (6.6 ft) from ground level may cause serious health effects (exceed the AEGL-2 level) up to approximately 84.2 ft (25.7 m) from the burning enclosure in a large fire scenario with high winds and a stable atmosphere. The modeled high wind speed was 16 mph (7.2 $\frac{m}{s}$), which is the 99th percentile wind speed for the Starlight site. Beyond approximately 84.2 ft (25.7 m), the carbon monoxide concentrations were below AEGL-2 levels for all fire scenarios considered. For first responders who may be operating within this region, guidance for appropriate personal protective equipment (PPE) may be found in relevant Emergency Response Protocol (ERP) documents.
- The Starlight site is in a relatively isolated location. The nearest exposure is approximately 1235 ft away from the nearest BESS enclosure. Single homes are scattered around the site with the nearest approximately 1331 ft away from the nearest BESS enclosure. An elementary school is located approximately 1.15 miles northwest of the nearest BESS enclosure. Based on the model results and the prevailing wind direction at the site, it is unlikely that nearby homes will experience toxic levels of carbon monoxide in the event of a single BESS unit experiencing a failure event.
- The hydrogen fluoride (HF) source term was estimated to be 43.5 mg/Wh based on literature values. However, HF was not measured during the cell-level, module-level, or unit-level UL 9540A testing for this system. In a separate test conducted using the UL 9540A unit-level method with additional gas collection beyond the standard test protocol, HF was measured in collected gas samples, indicating that HF generation can occur under similar failure conditions. HF has been measured in laboratory-scale battery thermal runaway tests; however, the range of reported measurements is wide. Thus, hydrogen fluoride may be a risk, but the exact magnitude of this risk is unknown. Hydrogen fluoride is highly reactive with a range of materials including metals and various organic compounds. It is unclear whether substantial HF concentrations persist at a distance away from larger module, rack, and BESS scales. HF can also be emitted from the combustion of plastic components in the BESS, such as wiring insulation and module or rack enclosure casings. Although these plastics are commonly fire-retarded, fire-retardant plastics can be overwhelmed if the severity of the fire is sufficiently large. Similar fire-retardant plastics are commonly found in non-battery applications and may pose similar emission hazards during fire conditions.

- The sulfur dioxide ($SO_2$) source term was assumed to be 28 mg/Wh based on literature values despite not being reported during testing for this system. ($SO_2$) is highly reactive with a range of materials including metals, oxygen and water vapor, and various organic compounds. It is unclear whether substantial ($SO_2$) concentrations persist at a distance away from larger module, rack, and BESS scales.
- Other toxic organic gases, such as volatile organic compounds (VOCs), make up only trace amounts of the battery vent gas. VOC release quantities are too small to exceed hazardous levels at any distance from the unit.

Note that this Executive Summary does not contain all of Hazard Dynamics' technical evaluations, analyses, conclusions, and recommendations. Hence, the main body of this report is at all times the controlling document.

# 2 Introduction

This report describes the results of a plume dispersion study conducted for the Starlight battery energy storage system (BESS), which is being constructed for Starlight Solar in Boulevard, California. A specific BESS manufacturer and enclosure model has not been selected at the time of this analysis; therefore, representative system characteristics were based on publicly available information for lithium-ion battery energy storage systems, with primary reference to data for the Tesla Megapack 2 XL. The purpose of a plume study is to identify and quantify potential risks associated with toxic gases produced by a BESS under abnormal conditions.

Where appropriate toxicity data is unavailable, reasonable engineering assumptions will be made based on the available body of technical literature. This analysis was conducted using a set of probable worst-case scenarios informed by publicly available data, including representative findings from UL 9540A testing and considering conditions up to a fully involved fire in a single unit. Project-specific UL 9540A reports were not available, as these are dependent on the selected BESS manufacturer, which has not yet been determined; therefore, publicly available information was used to develop conservative assumptions.

This report will first provide background on the toxicity hazards of lithium-ion battery systems. Next, it will review the details of the Starlight site as well as the energy storage system itself. Finally, the report will evaluate possible toxic gas release scenarios and their consequences.

This analysis relies on the following information:

- Plans for the Starlight site [1][2]
- Tesla, Inc. Megapack 2 XL Datasheet dated 2/10/2023 [3]
- Tesla, Inc. Megapack 2 XL Safety Overview dated 9/13/2022 [4]
- Tesla Pre-PO Engineering Review Requirements by Energy Toolbase [5]
- Fire Protection and Engineering Analysis for the Tesla, Inc. Megapack 2 XL by Fisher Engineering, Inc. report number 22035 dated 1/23/2023 [6]
- Battery Energy Storage System Preliminary Fire Risk Assessment and Heat Flux Analysis by Hiller Companies dated 7/23/2025 [7]

# 3 Background on Lithium-Ion ESS Toxicity Hazards

## 3.1 Toxicity Hazards

Toxicity hazards may exist alone or in combination with fire and explosion hazards. A significant amount of the gas released during thermal runaway is carbon monoxide (CO), which is toxic. Depending on the conditions, the combustion of battery gases may burn off some carbon monoxide or create additional carbon monoxide from partially reacted hydrocarbons. Smaller amounts of other toxic gases may also be released depending on the cell, whether the gases burn, and if water or other suppression agents are added. Experiments show that lithium-ion cells in thermal runaway may release hydrogen fluoride (HF), hydrogen chloride (HCl), hydrogen cyanide (HCN), nitrogen dioxide ($NO_2$), sulfur dioxide ($SO_2$), and other gases [8]. When the gases burn, some of the toxic components may be consumed, although others may be generated. Smoke from many fires, including battery fires, is considered hazardous. Smoke typically includes asphyxiant gases, irritant toxic gases, and particulate matter. The introduction of water to a fire may change the composition of the smoke and can create water runoff, which may also contain hazardous substances. The use of other fire suppression agents may also alter the toxic release profile [9].

## 3.2 Toxic Gases of Interest

Abuse and failure of lithium-ion cells may result in gas production inside of the cells. When enough gas is produced, a safety vent may open, or the cell package may rupture. The gas mixture released is flammable and toxic and is primarily made up of carbon monoxide (CO), carbon dioxide ($CO_2$), hydrogen ($H_2$), and an assortment of hydrocarbons. If ignited, the combustion of these gases can lead to a fire or an explosion.

When a lithium-ion cell is exposed to high temperatures such as those due to fire exposure or propagating thermal runaway, it produces toxic compounds. Plastic contained in the battery system may contribute to these toxic combustion products. Such products may include carbon monoxide (CO), nitrogen oxides ($NO_x$), sulfur dioxide ($SO_2$), hydrogen chloride (HCl), and hydrogen fluoride (HF). The quantity of HF produced is related to the electrolyte solvent and the chemical reactions initiated. $CO_2$, $H_2$, and $CH_4$ are asphyxiant gases, or gases that can cause unconsciousness or death by suffocation because they displace oxygen in the air [8]. CO blocks the transport of oxygen by sticking to the hemoglobin in red blood cells. Poisoning by CO is often the major cause of death related to fire in which burns are not present [10]. Hydrogen cyanide (HCN) obstructs the function of mitochondria so that oxygen cannot be absorbed into the cells. Irritant gases include HF, HCl, $SO_2$, and $NO_2$. These gases have a toxic and irritating effect that can be significant even at very low concentrations. HCl is corrosive, highly irritating, and can cause severe injury to the respiratory tract if inhaled. $SO_2$ is extremely irritating and can form sulfurous acid when in contact with moisture. $NO_2$ and NO are especially irritating to the respiratory tract and lungs even at low concentrations. None of these irritants can be absorbed through the skin. HF, on the other hand, is not only severely irritating to the respiratory tract but can also penetrate skin and other tissues as the fluoride ion. When HF comes into contact with moisture, it can form hydrofluoric acid [11].

In evaluating harmful levels of toxic gases, it is helpful to reference levels known as IDLH (immediately dangerous to life or health) and AEGLs (acute exposure guideline levels). According to the Code of Federal Regulations, IDLH is defined as a concentration of any toxic, corrosive, or asphyxiant substance that poses an immediate threat to life, would cause irreversible or delayed adverse health effects, or would interfere with an individual's ability to escape from a dangerous atmosphere [11]. IDLH values were developed to address occupational exposures to chemicals and to help protect workers from acute or short-term exposures to high concentrations of some airborne chemicals that could result in undesirable health outcomes [12]. The AEGLs were developed by the EPA to define the health effects of a once-in-a-lifetime exposure to airborne chemicals. AEGLs are used by emergency responders when dealing with major chemical leaks, spills, or other exposures. AEGL concentrations are provided for different exposure times and

health effect levels. Level 1 is discomfort or irritation, Level 2 is the onset of irreversible or serious health effects, and Level 3 describes life-threatening health effects [13]. Toxic gases related to battery energy storage systems along with their IDLH, AEGL-2, and AEGL-1 concentrations are shown in Table 1. The AEGL values presented in the table are based on an exposure time of 30 minutes, which is characteristic of how long someone evacuating might be exposed to a substance. This characteristic time is a reasonable upper bound for emergency responders; however, evacuation times may vary depending upon the incident environment.

Table 1: Toxic chemicals that can be present during battery failure and concentrations of interest. The AEGL values shown are for a 30-minute exposure. (NR = Not recommended due to insufficient data)

| Chemical | IDLH (ppm) | AEGL-3 (ppm) | AEGL-2 (ppm) | AEGL-1 (ppm) |
|---|---|---|---|---|
| **Carbon Monoxide (CO)** | 1,200 | 600 | 150 | NR |
| **Carbon Dioxide ($CO_2$)** | 40,000 | NR | NR | NR |
| **Hydrogen Chloride (HCl)** | 50 | 210 | 43 | 1.8 |
| **Hydrogen Cyanide (HCN)** | 50 | 21 | 10 | 2.5 |
| **Hydrogen Fluoride (HF)** | 30 | 62 | 34 | 1 |
| **Nitrogen Dioxide ($NO_2$)** | 13 | 25 | 15 | 0.50 |
| **Nitric Oxide (NO)** | 100 | NR | NR | NR |
| **Sulfur Dioxide ($SO_2$)** | 100 | 30 | 0.75 | 0.20 |
| **Benzene ($C_6H_6$)** | 500 | 5,600 | 1,100 | 73 |
| **Toluene ($C_6H_5CH_3$)** | 500 | 5,200 | 760 | 67 |

# 4 Site Description

The Starlight project is a photovoltaic and lithium-ion BESS facility that will be located in Boulevard, California. The site will be located approximately 3 miles north of the United States-Mexico border. The location of the site can be seen in Figure 1.


Figure 1: A map showing the location of the Starlight site. This image was taken from Google Maps 2026.

The Starlight project will include lithium-ion battery energy storage equipment. The site is in a relatively isolated location. The nearest exposure is approximately 1235 ft away from the nearest BESS enclosure. Single homes are scattered around the site as shown in Figure 2. Nearby exposures and their approximate distances from the BESS are also shown in Figure 2. Notably, an elementary school is located approximately 1.15 miles northwest of the nearest BESS enclosure (not shown in the figure).

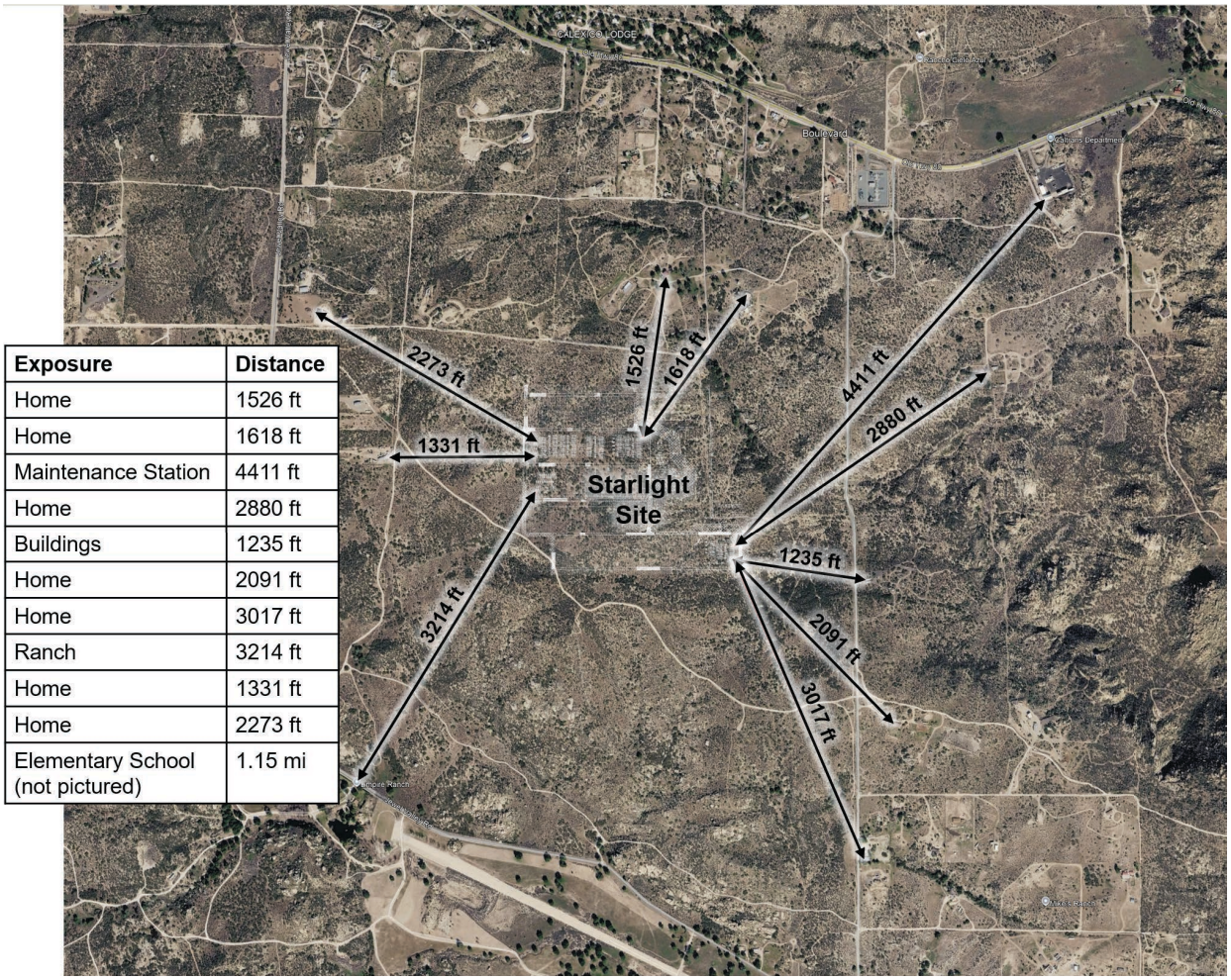


| Exposure | Distance |
|---|---|
| Home | 1526 ft |
| Home | 1618 ft |
| Maintenance Station | 4411 ft |
| Home | 2880 ft |
| Buildings | 1235 ft |
| Home | 2091 ft |
| Home | 3017 ft |
| Ranch | 3214 ft |
| Home | 1331 ft |
| Home | 2273 ft |
| Elementary School (not pictured) | 1.15 mi |

Figure 2: A satellite view of the Starlight site location and its surroundings with the site drawing overlaid. The distances shown are measured from the nearest BESS enclosure. This image was produced using Google Earth.

## 4.1 Typical Wind Conditions

Wind conditions can affect the behavior of a toxic plume or fire. In windy conditions, it is expected that the most severely impacted area would be downwind of the site. Historical wind data was taken from the Boulevard weather station, which is near the Starlight site. According to historical wind information from 2010-2025, the prevailing winds generally come from the west-southwest, with a significant amount coming from the northeast (see Figure 3). The average wind speed is 4.5 mph or 2 $\frac{m}{s}$. Conditions are calm 23.5% of the time [14]. The wind data was analyzed to find the 99th percentile wind speed for use in the CFD model. This wind speed was found to be 16 mph or 7.2 $\frac{m}{s}$.

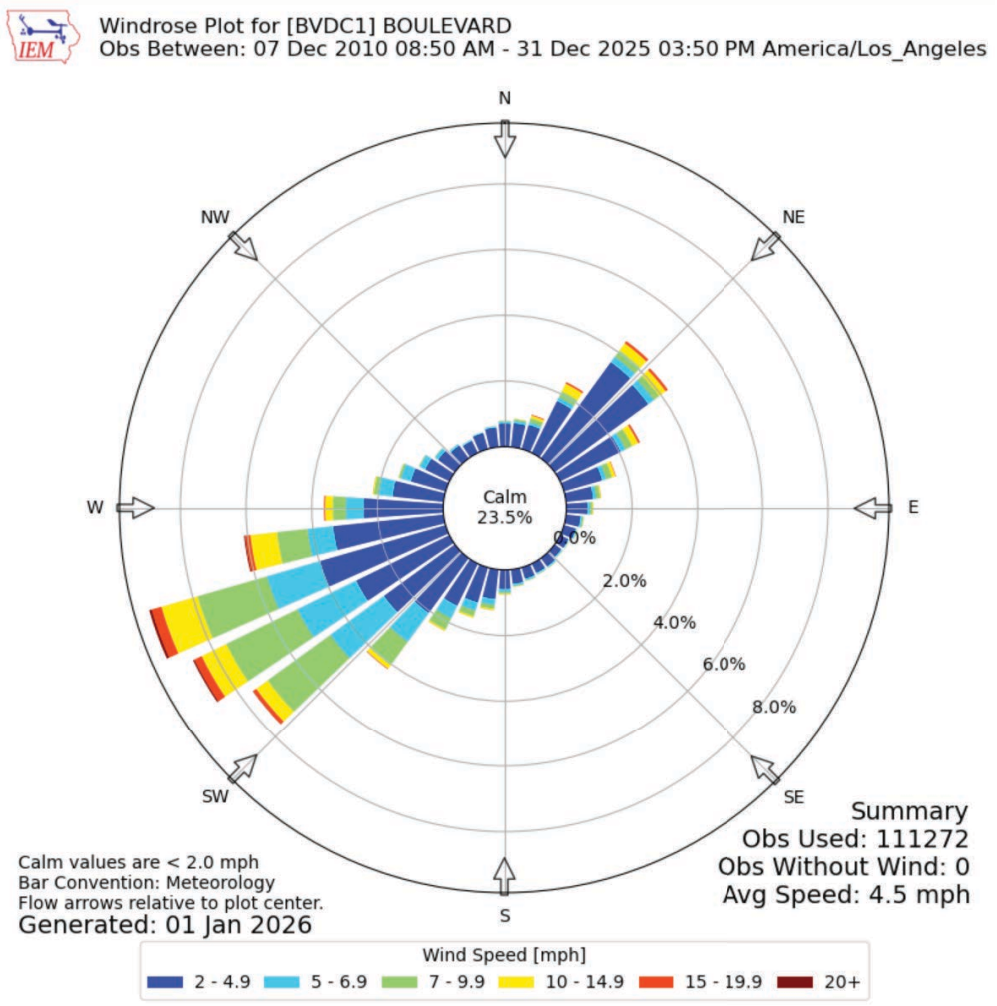


Figure 3: The wind rose for the Boulevard weather station, which is near the Starlight site. This image was taken from the Iowa State University Iowa Environmental Mesonet website [14].

## 4.2 BESS Layout

The project will be split into two phases. The first phase will be located on 125.01 ac of land and will include 17.4 MW of lithium-ion battery energy storage equipment, while the second phase will be located on 455.94 ac of land and will include 200 MW of energy storage [2]. The site also includes photovoltaic panels, power conversion systems, and other equipment. Figure 4 shows the proposed layout for the Starlight site [1].

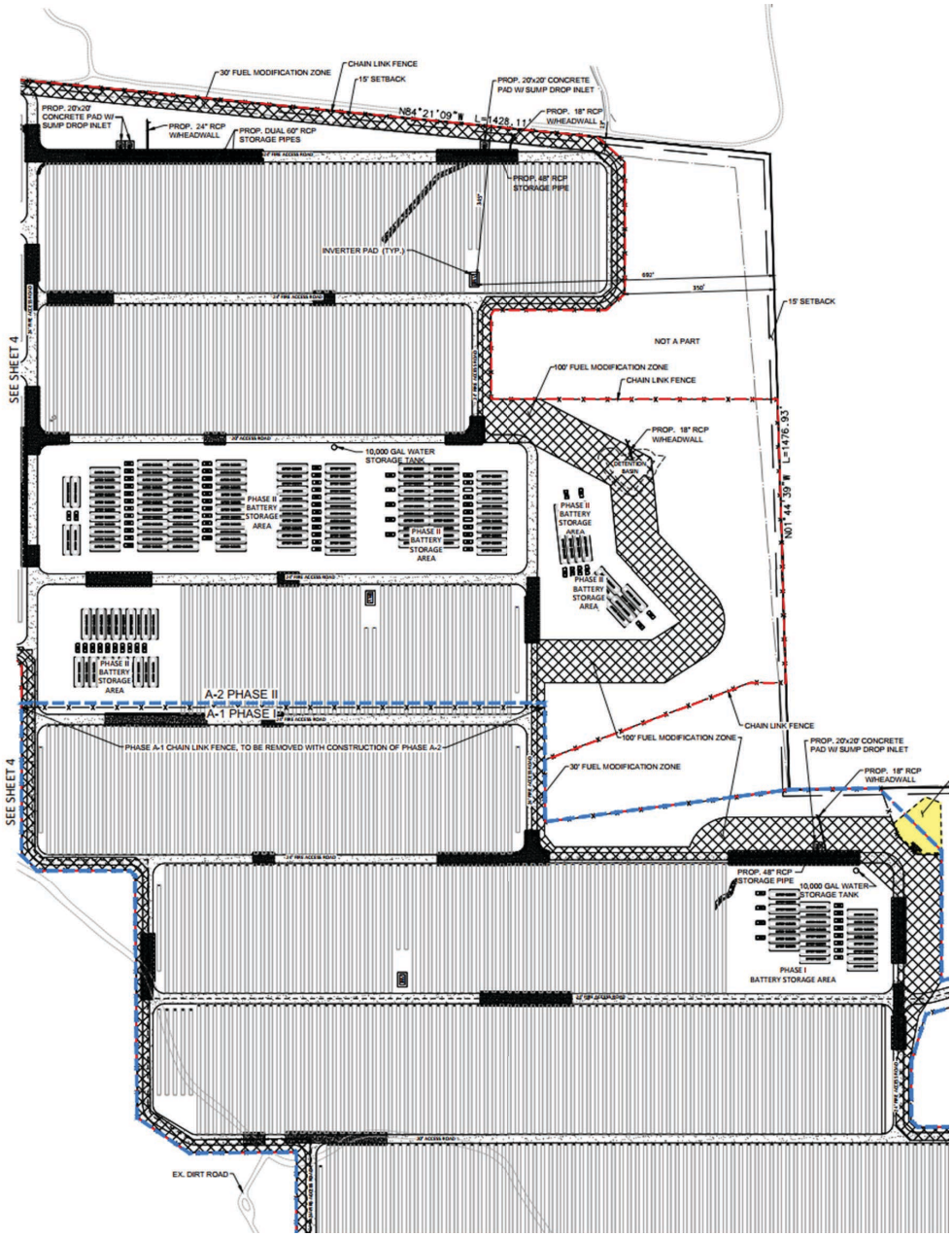


Figure 4: An engineering drawing indicating the planned layout of the Starlight site, including the photovoltaic panels, battery enclosures, power conversion systems, and other equipment [1].

# 5 Energy Storage System Description

The Starlight project will utilize modular, outdoor-rated lithium-ion battery enclosures; however, a specific manufacturer has not yet been selected. For the purposes of this analysis, the physical specifications of the units were modeled based on the Tesla, Inc. Megapack 2 XL. These units contain Contemporary Amperex Technology Co., Ltd. (CATL) lithium-ion batteries installed in racks inside the enclosure. Each enclosure contains 24 liquid-cooled battery modules. The Megapack 2 XL includes battery modules with active and passive fuses, a touch-safe customer

interface bay, a non-walk-in IP66 enclosure with deflagration mitigation, and a thermal roof with overpressure vents [4]. Significantly, the Megapack 2 XL contains sparkers that are installed in a variety of locations and heights to ignite battery gas before it can accumulate [6]. A Megapack 2 XL enclosure is shown in Figure 5.

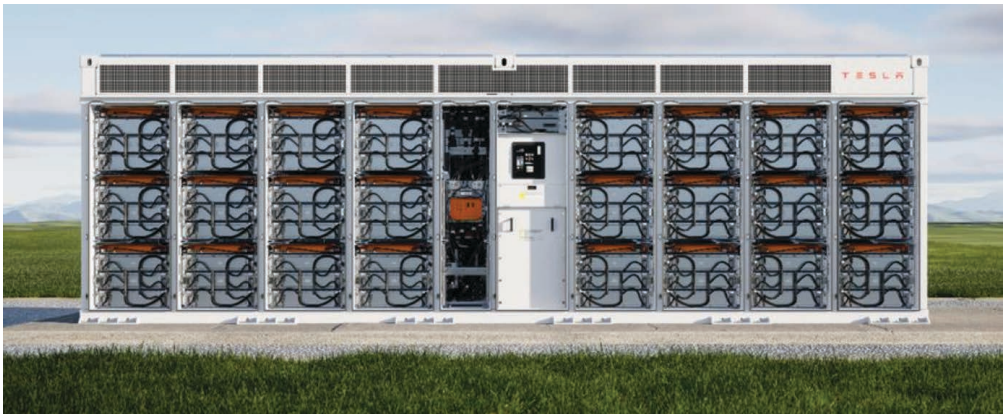


Figure 5: An image of a Tesla, Inc. Megapack 2 XL battery storage system. [6].

## 5.1 System Comparison

The Tesla Megapack 2 XL and Wärtsilä GridSolv Quantum are both utility-scale battery energy storage systems utilizing lithium iron phosphate (LFP) battery chemistry and are broadly comparable at the installation level in terms of deployed energy capacity and system application. While the individual enclosure designs differ in form factor and modularity, both systems are intended to be deployed in multi-unit configurations to achieve site-scale energy storage requirements.

The Megapack 2 XL is a large, fully integrated enclosure (approximately 8.8 m wide) with a per-unit energy capacity of approximately 3,854-3,916 kWh, whereas the GridSolv Quantum is a smaller modular enclosure (approximately 2.1 m wide) with a nominal per-unit capacity of approximately 1,300-1,490 kWh [3]. Although the GridSolv system consists of smaller individual units, these are typically deployed in grouped configurations with up to eight enclosures conjoined to form larger integrated blocks (up to 11.92 MWh) as seen in Figure 6 [15]. The Megapack 2 XL, on the other hand, can be deployed as two back-to-back enclosures (up to 7.83 MWh). As a result, both technologies achieve comparable utility-scale deployments.

Figure 6: Two physically connected Wärtsilä GridSolv Quantum enclosures installed in a modular configuration, illustrating how units are combined to form a larger system. This image was taken from the Wärtsilä GridSolv Quantum Specification Sheet [15].

The Megapack 2 XL includes a sparker system that is designed to ignite flammable gas released during battery thermal failures and to exhaust the resultant combustion products and flames through the roof [6]. The Wärtsilä GridSolv Quantum deploys a different safety mitigation approach, where deflagration panels are installed on the roof and an optional ventilation exhaust system can be integrated into the side doors [15]. For fire conditions–especially large fires– the deflagration panels are likely to have opened, and fire is expected to be released through the panels on the top of the unit. Fire may also escape through failed door seals for both the Megapack 2 XL and the GridSolv Quantum. While the physical enclosure geometries differ, both systems are assumed to exhibit similar fire development behavior in terms of flame and plume release, with combustion products expected to vent predominantly from the upper portion of the enclosure in a fire scenario.

For the purposes of this analysis, fire hazard characterization is governed primarily by the assumed heat release rate (HRR), which is the dominant driver of plume rise, dispersion, and resulting downwind toxic gas concentrations. The peak HRR for both the Megapack 2 XL and GridSolv Quantum were estimated and compared. For BESS with similar battery chemistry, the total heat released during a fire is expected to scale with the total energy of the unit. The HRR profile will also depend on the fire growth rate. The HRR profile for the Megapack 2 XL was estimated based on fire growth rate observations from large scale testing summarized in the Fisher Engineering, Inc. *Fire Protection and Engineering Analysis* report [6]. Details regarding the method used to estimate the HRR profile are provided in Section 8 and the Appendix. The peak HRR for the GridSolv Quantum was taken from the *Preliminary Fire Risk Assessment and Heat Flux Analysis* conducted by Hiller Companies [7]. To be conservative, the larger peak HRR estimate was assumed to be the basis for the fire scenarios considered in this plume study.

The Tesla Megapack geometry is used as the representative physical enclosure configuration for dispersion and spacing considerations. This selection is based on its widespread deployment, the availability of relatively detailed publicly available information on its configuration, and its expected likelihood of selection for use at the Starlight project site. Given that both systems are of comparable installation-scale class, the Megapack 2 XL configuration is considered a reasonable surrogate for spatial layout and enclosure footprint representation in the absence of a final technology selection. Using the Megapack geometry while applying the more conservative Wärtsilä HRR therefore provides a consistent and conservative modeling framework.

# 6 UL 9540A Testing

This analysis would typically be based on test data from UL 9540A cell-level, module-level, and unit-level testing. However, project-specific UL 9540A reports were not provided for this project because an original equipment manufacturer (OEM) has not been finalized. Currently, a Tesla system is being considered the most likely for use at the Starlight site. The Fisher Engineering, Inc. *Fire Protection and Engineering Analysis* report for the Tesla, Inc. Megapack 2 XL was found to be publicly available. This report provides a summary of cell-level, module-level, and unit-level test results which will be used for this analysis [6]. During UL 9540A testing, a cell is forced into thermal runaway while the outcome is observed, and gases released from the battery or batteries are captured and analyzed for select chemical species. Depending on the outcome of cell-level testing, additional testing at the module and full unit levels may also be conducted. For this plume analysis, the summarized results presented in the Fisher Engineering, Inc. report, which include representative cell-level, module-level, and unit-level testing, were reviewed [6]. These results are described in Sections 6.1-6.3.

Since UL 9540A is primarily concerned with fire and explosion hazards, typical UL 9540A gas measurements are focused on major combustible gases and combustion products, such as hydrogen, carbon monoxide, carbon dioxide, and various hydrocarbons. Typically, carbon monoxide is the most significant toxicity hazard among the measured gases due to a comparatively low IDLH value and relative abundance in most battery gas. The available summary of UL 9540A testing for the Contemporary Amperex Technology Co., Ltd. (CATL) cells indicates that, of the gas captured during testing, 10.9% by volume was carbon monoxide. This information, along with the remaining composition information, is listed in Table 3.

Cell-level gas composition information is collected by failing an individual cell inside of a sealed pressure vessel that is filled with an inert gas to prevent combustion. This method allows for the capture of the entire volume of emitted gas. Gas compositions from cell experiments are usually measured using a gas chromatograph (GC), which is typically more accurate than measurements taken from exhaust hoods during module and unit testing.

## 6.1 Cell Test

The system under consideration is comprised of Contemporary Amperex Technology Co., Ltd. (CATL) cells, which are 157.2 Ah lithium-ion LFP cells [6]. This cell was tested using the UL 9540A method. The results are given in the UL report dated 12/2021, as summarized in the Fisher Engineering, Inc. *Fire Protection and Engineering Analysis* report [6]. Figure 7 shows a cell with measuring tapes for scale.

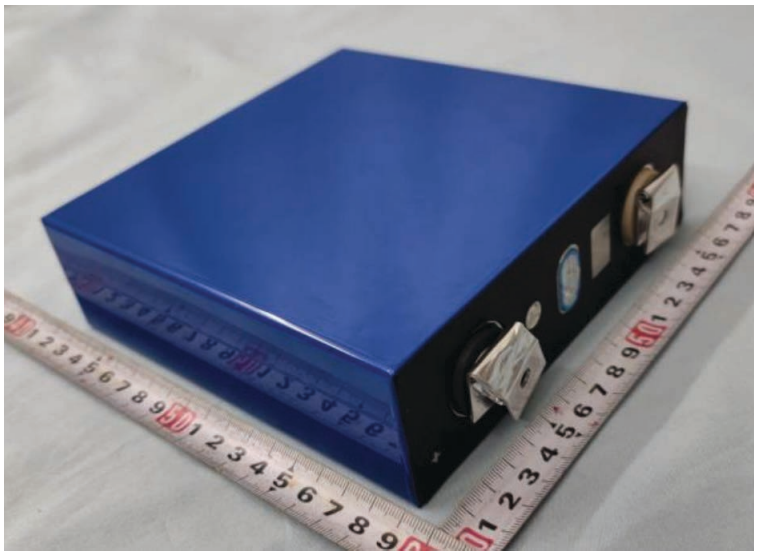

Figure 7: A Contemporary Amperex Technology Co., Ltd. (CATL) cell with measuring tapes for scale. This image was taken from the Fisher Engineering, Inc. report [6].

For UL 9540A testing, the cells were heated until failure occurred. Cell details are provided in Table 2.

Table 2: Key cell properties from the UL 9540A cell test [6].

| Parameter | Value |
|---|---|
| **Cell Manufacturer** | Contemporary Amperex Technology Co., Ltd. (CATL) |
| **Cell Chemistry** | LFP |
| **Cell Nominal Voltage** | 3.22 V |
| **Cell Capacity** | 157.2 Ah |

The Fisher Engineering, Inc. report states that the cells released a mixture of flammable gases when heated externally until failure. The vent gas composition from the UL 9540A cell report is listed in Table 3.

Table 3: The gas composition from the UL 9540A cell test [6]. Model Volume Percent will be addressed in Section 8 later in this document.

| Name | Formula | Experimental Volume Percent | Model Volume Percent |
|---|---|---|---|
| **Carbon Monoxide** | $CO$ | 10.881 | 10.881 |
| **Carbon Dioxide** | $CO2$ | 27.107 | 27.107 |
| **Hydrogen** | $H2$ | 50.148 | 50.148 |
| **Methane** | $CH4$ | 6.428 | 6.428 |
| **Acetylene** | $C2H2$ | 0.264 | 0.000 |
| **Ethylene** | $C2H4$ | 3.283 | 3.283 |
| **Ethane** | $C2H6$ | 1.100 | 1.100 |
| **Propene** | $C3H6$ | 0.379 | 0.000 |
| **Propane** | $C3H8$ | 0.125 | 1.053 |
| **C4 Total** | $C4H10$ | 0.190 | 0.000 |
| **C5 Total** | $C5H12$ | 0.027 | 0.000 |
| **C6 Total** | $C6H14$ | 0.005 | 0.000 |
| **Benzene** | $C6H6$ | 0.002 | 0.000 |
| **Toluene** | $C7H8$ | 0.002 | 0.000 |
| **Dimethyl Carbonate** | $C3H6O3$ | 0.055 | 0.000 |
| **Ethyl Methyl Carbonate** | $C4H8O3$ | 0.004 | 0.000 |

## 6.2 Module Test

The Contemporary Amperex Technology Co., Ltd. (CATL) cells are arranged within modules composed of three trays per module. The UL 9540A testing was performed on a representative portion of a module consisting of a single tray containing 112 cells. The results are documented in the TUV SUD (TUV) test report dated 05/2022, as summarized in the Fisher Engineering, Inc. *Fire Protection and Engineering Analysis report* [6]. Multiple thermocouples were attached as shown in Figure 8.

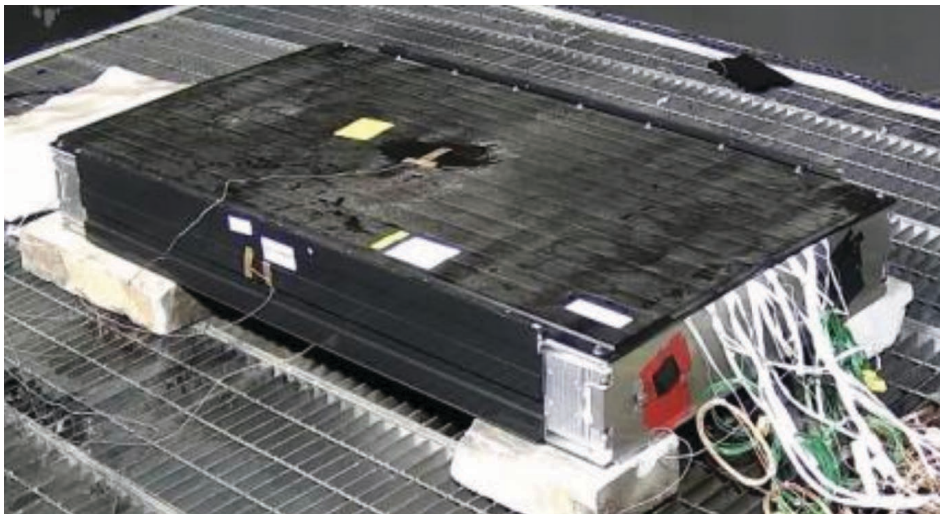

Figure 8: A module prepared for the UL 9540A test. This image was taken from the Fisher Engineering, Inc. report [6].

Film strip heaters were installed on both sides of two initiating cells. The initiating cells were heated until thermal runaway occurred. Thermal runaway propagated through the entire tray, resulting in failure of all 112 cells [6]. Sparks, flying debris, and external flaming were observed during the test.

## 6.3 Unit Test

The UL 9540A unit test for unit model MP2 is described in Northern Nevada Research Center report dated 3/9/2022 and summarized in the Fisher Engineering, Inc. *Fire Protection and Engineering Analysis report* [6]. In this test, a unit comprised of 19 modules was tested. The unit contained 6384 individual cells [6]. The initiating tray, containing six cells equipped with four film heaters, was positioned between two adjacent trays within a module. This module was then installed within a full unit, which was placed in proximity to walls and target units. The configuration of the initiating tray is shown in Figure 9, the configurations of the initiating module and unit are shown in Figure 10, and a diagram of the test setup is shown in Figure 11.

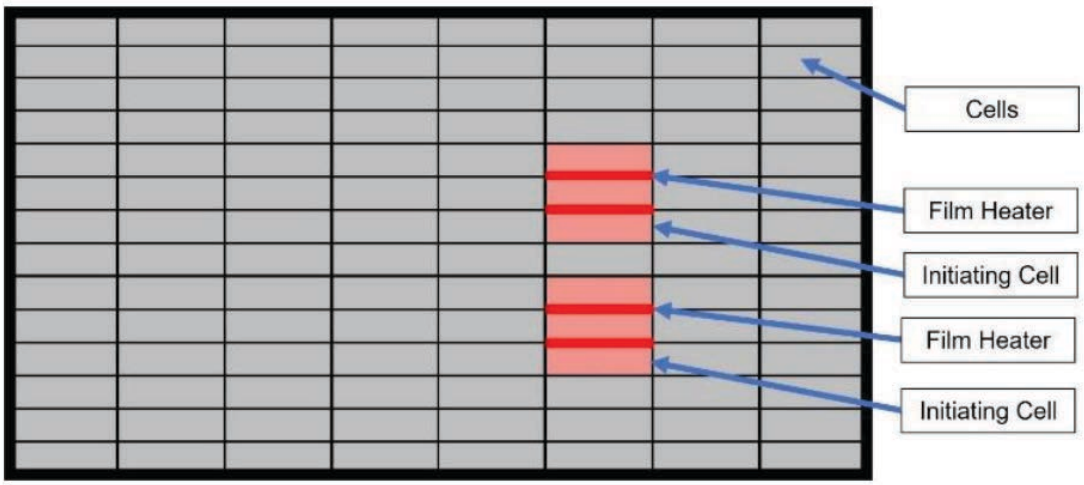


Figure 9: A diagram of the initiating tray setup for the UL 9540A test. This image was taken from the Fisher Engineering, Inc. report [6].

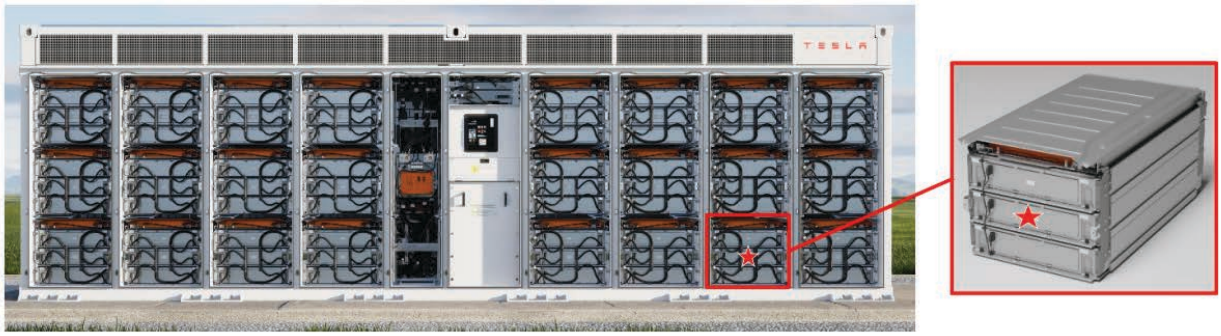

Figure 10: The initiating unit with the placement of the initiating tray and module highlighted. This image was taken from the Fisher Engineering, Inc. report [6].

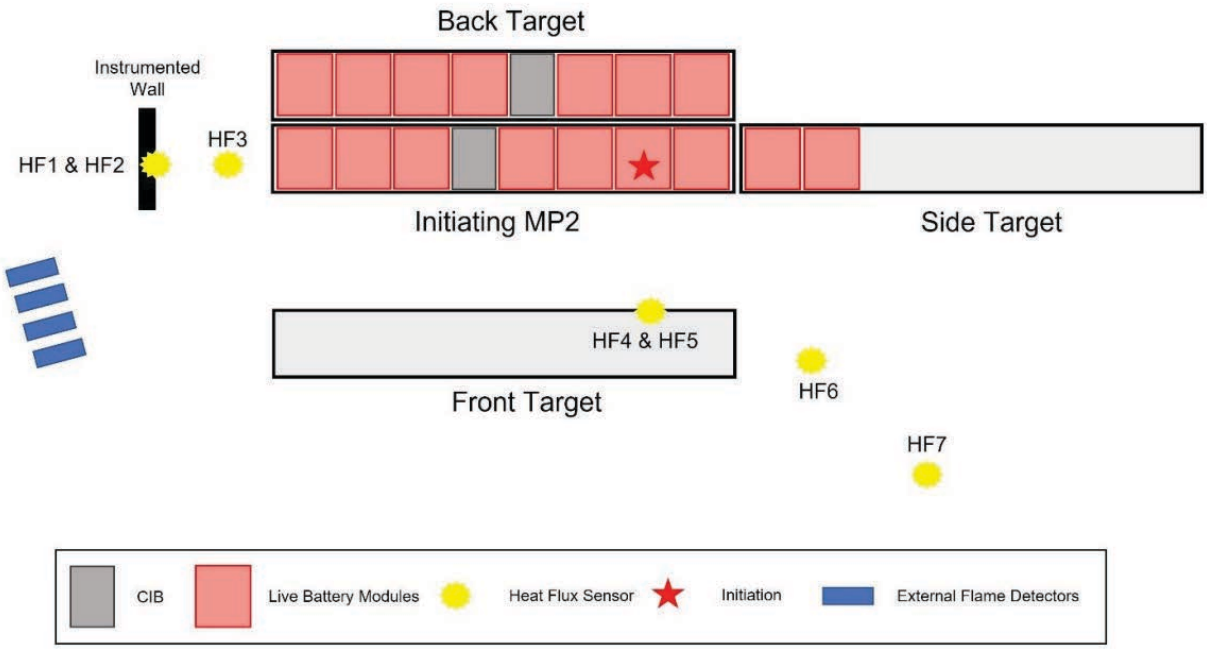


Figure 11: A diagram of the unit test setup. This image was taken from the Fisher Engineering, Inc. report [6].

Thermal runaway was initiated by activating the heaters on the six initiating cells in the initiating module. Once thermal runaway began, the power to the heaters was disconnected. Thermal runaway continued to propagate until a total of seven cells inside the initiating module had failed [6]. Thermal runaway did not propagate to other modules in the unit or to other units. White smoke was seen intermittently during the test [6].

# 7 Large-Scale Fire Test

Tesla performed a large-scale fire test (LSFT) on a fully-populated Megapack 2 XL at 100% state of charge on May 19, 2022. This test was intended to cause a severe failure of the system. The test and its results are summarized in the Fisher Engineering, Inc. report entitled *Fire Protection Engineering Analysis* dated January 23, 2022 [6]. Information from this test was used to help approximate a large fire scenario.

In order to test for a severe failure, 32 film heaters were installed in tray 2 of a 3-tray module. The positions of these heaters within the initiating tray are shown in Figure 12. This initiating module was then inserted into a full unit in the position shown in Figure 13 [6].

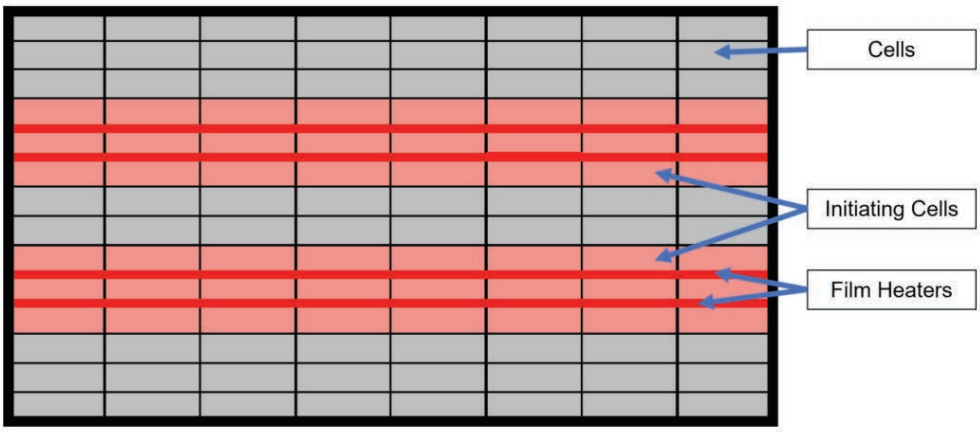


Figure 12: The heaters used within the initiating module to cause a severe failure of the Megapack 2 XL [6].

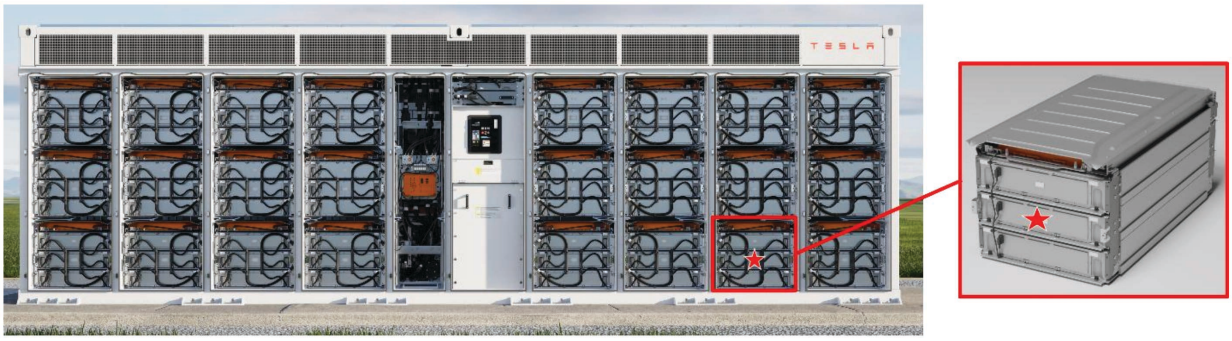

Figure 13: The location of the initiating module within the Megapack 2 XL during testing [6].

Thermal runaway was initiated in the cells adjacent to the heaters in the initiating module. Failure then propagated through all battery bays on one side of the Customer Interface Bay, which is in the center of the enclosure, as described in Figure 14. Pictures taken during the test are shown in Figure 15 [6].

| Approximate Elapsed Time hr:min:sec | Event |
|---|---|
| **00:00:00** | **Start of Test. Cameras, DAQ and heaters turned on.** |
| 0:40:44 | First thermal runaway confirmed. |
| 1:14:08 | An overpressure event occurred. An overpressure vent opened, and the cabinet doors remained closed. Smoking observed. |
| 1:24:00 | Flames observed predominantly coming out the front doors of the cabinet and out the front grill of the thermal roof (just above the doors). |
| 2:30:00 | Flames spread to the adjacent battery bays 8 and 10. Approximate peak flame intensity. |
| 4:00:00 | Flames spread to adjacent battery bay 7. |
| 8:04:00 | Flaming ceases. Flames did not spread to any other battery bays.<br>**End of Test.** |

Figure 14: A summary of the LSFT on the Megapack 2 XL [6].

Figure 15: Pictures taken during the LSFT of the Megapack 2 XL [6].

# 8 Fire and Toxicity Modeling

Hazard Dynamics used data from the UL 9540A test reports, as summarized in the Fisher Engineering, Inc. report, to conduct plume modeling for a number of different failure scenarios. These models included cases of varying wind conditions, differing levels of failure severity, and atmospheric stability classes ranging from D to F. Gas release scenarios in the absence of burning were not modeled because the Megapack 2 XL contains a sparker system that is designed to ignite battery vent gas before it can be released outside of the BESS enclosure[6].

Two heat release rates (HRRs) were used to represent different fire sizes. The larger HRR, 16.4 MW, represents a full enclosure fire. Although a BESS manufacturer has not been selected at this stage, the Tesla, Inc. Megapack 2 XL was used as the basis for physical assumptions in this analysis. A full enclosure fire HRR based on the Tesla, Inc. Megapack 2 XL was estimated using cell-level and module-level data from UL 9540A testing, as summarized in the Fisher Engineering, Inc. *Fire Protection Engineering Analysis* report [6]. The HRR profile was developed using the fire duration observed in the large-scale fire test documented in the same report, resulting in an estimated HRR of 8.81 MW. Here, a simple trapezoidal fire profile was assumed where the time to peak heat release rate, a constant peak release rate, and a decay time were used to parameterize the profile. Additional details regarding this calculation are provided in the Appendix. However, the *Preliminary Fire Risk Assessment and Heat Flux Analysis* conducted by Hiller Companies, which was based on a Wärtsilä GridSolv Quantum-type system, calculated a representative HRR of 16.4 MW [7]. In this study, the more conservative, i.e. larger, HRR value estimate for the Wärtsilä GridSolv Quantum-type system was assumed as the worst-case heat release for the large fire scenarios, which effectively provides a nearly 2x conservative safety factor. Flaming propagation between adjacent enclosures was not modeled as available UL 9540A test data did not demonstrate propagation between modules inside of a unit or between units. The small HRR of 1.64 MW was taken to be 10% of the large fire. This HRR was used to evaluate the consequences of a smaller fire in which the entire enclosure does not burn.

Each scenario assumes a steady-state release and was modeled for 300 seconds. The scenarios are summarized in Table 4. The atmospheric stability classes and wind speeds used in the models will be discussed in Section 8.1.

Table 4: Starlight plume model scenarios

| Name | Wind Speed | Mass Release Rate | HRR |
|---|---|---|---|
| **Large Fire High Wind, Stable (F)** | 7.2 $\frac{m}{s}$ | 1.13 $\frac{kg}{s}$ | 16.4 MW |
| **Large Fire High Wind, Slightly Stable (E)** | 7.2 $\frac{m}{s}$ | 1.13 $\frac{kg}{s}$ | 16.4 MW |
| **Large Fire High Wind, Neutral (D)** | 7.2 $\frac{m}{s}$ | 1.13 $\frac{kg}{s}$ | 16.4 MW |
| **Large Fire Low Wind, Stable (F)** | 1.5 $\frac{m}{s}$ | 1.13 $\frac{kg}{s}$ | 16.4 MW |
| **Large Fire Low Wind, Slightly Stable (E)** | 1.5 $\frac{m}{s}$ | 1.13 $\frac{kg}{s}$ | 16.4 MW |
| **Large Fire Low Wind, Neutral (D)** | 1.5 $\frac{m}{s}$ | 1.13 $\frac{kg}{s}$ | 16.4 MW |
| **Small Fire High Wind, Stable (F)** | 7.2 $\frac{m}{s}$ | 0.113 $\frac{kg}{s}$ | 1.64 MW |
| **Small Fire Low Wind, Stable (F)** | 1.5 $\frac{m}{s}$ | 0.113 $\frac{kg}{s}$ | 1.64 MW |

For modeling purposes, the most significant components which account for more than 95% of the gas are modeled in the gas release mixture, while minor hydrocarbon elements are approximated as propane. The volume percents used in the model can be found in column four of Table 3.

## 8.1 Model Setup

The plume model uses grid sizes ranging from 0.25 m (9.8 in) to 2 m (6.6 ft) to capture both the flow near the source (starting 2 m from the enclosure) as well as the dispersion over a large flat downwind area up to 320 m (1050 ft) away from the source. Each grid element is assumed to be cubic with the same spatial dimensions in all three cartesian coordinates. Multiple BESS enclosures were modeled to evaluate their effect on the wind profile and dispersion of the plume. Only the enclosure furthest downwind was modeled as being on fire. Based on previous work, the presence of downwind structures similar in size to the BESS enclosure reduces the aerodynamic downwash downwind of the incident BESS enclosure and effectively prevents the plume from bending toward the ground, which would result in reduced plume concentrations at the ground level. Therefore, modeling the furthest downwind enclosure is expected to

be the worst-case condition because it is the closest enclosure to downwind exposures outside the site property line, and it is expected to exhibit increased aerodynamic downwash compared to enclosures further upwind. For the high wind large fire scenarios, the modeled domain was extended to 1500 m (4920 ft) to capture the increased distance traveled by the plume. Grid refinement studies were performed to ensure that these model domains are appropriate for use in this context. All mesh boundaries were modeled as open except the ground, which was modeled as closed. Figure 16 shows the model domain used for small fire scenarios with high wind conditions; in the large fire, high wind scenarios, the domain extends further downwind than is shown in the figure. Figure 17 shows the model domain used for fire scenarios with low wind conditions. The domain heights vary in order to capture plume behavior for each wind condition, with the low-wind domain extending higher and including a 2 m (6.6 ft) top mesh to capture the more vertically rising plume. For clarity, the computational grid itself is not displayed in the figures, as doing so would obscure important features; instead, the domain extents (mesh frames) are shown to illustrate the size and configuration of the modeled areas. Concentrations were measured across the full width of the domain at elevations of 2 m (6.6 ft) and 5 m (16.4 ft).

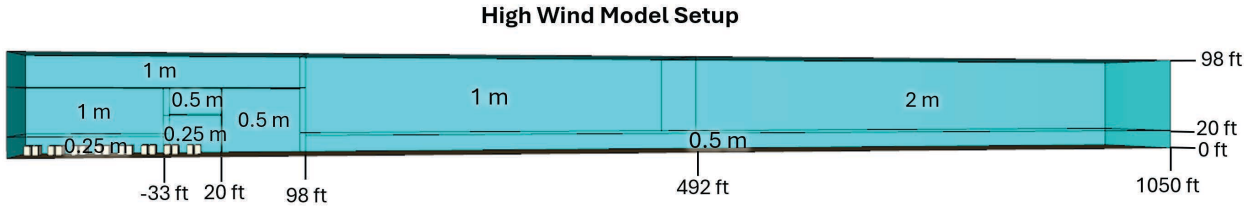


Figure 16: The model domain used for the small fire high wind simulation with the mesh extents and grid sizes shown. The grid resolution varies from 0.25 m near the unit to 2 m beginning approximately 492 ft from the enclosure. Vertically, the mesh resolution is refined to 0.5 m up to a height of 16 ft to better capture near-ground plume behavior. For the high wind large fire scenarios, the modeled domain was extended to 4920 ft to capture the increased distance traveled by the plume. Under higher wind speeds, the plume is bent downwind, allowing a model domain that is shorter in length. Distances shown are measured from the front of the enclosure.

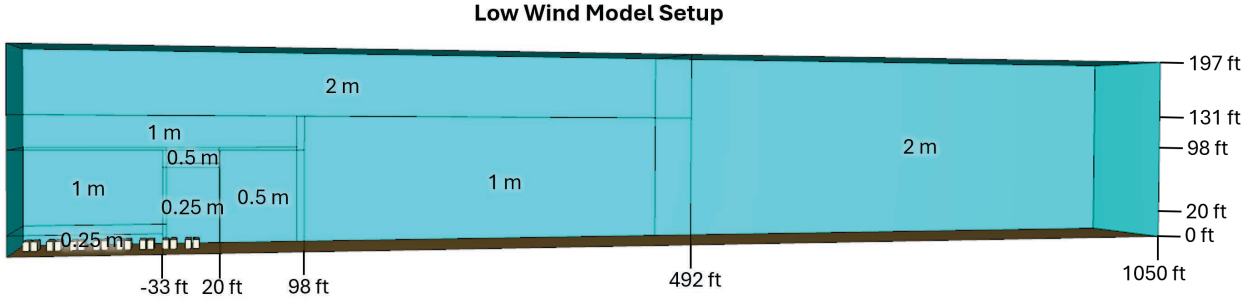


Figure 17: The model domain used for the low wind simulations with the mesh extents and grid sizes shown. The grid resolution varies from 0.25 m near the unit to 2 m beginning approximately 492 ft from the enclosure. Under lower wind speeds, the plume rises more vertically, requiring a model domain that is approximately twice as tall to capture the full plume development, with the upper portion of the domain using a 2 m grid resolution. Distances shown are measured from the front of the enclosure.

In the large fire scenarios, combustion product release was modeled to be consistent with observations from the large-scale fire documented in the Fischer Engineering report, in which

flames were observed issuing from the doors and the top of the enclosure [6]. To represent this behavior, releases were distributed across multiple vents, including along the top of the door seal (to represent burn-through at the doors) and on the top of the enclosure. In the small fire scenarios, the release was reduced to a limited area of these vents to represent a fire confined to a single rack, rather than the full enclosure.

The EPA Risk Management Program recommends using a wind speed of 1.5 m/s (3.4 mph) and atmospheric stability class F (stable conditions) for worst-case plume analysis of accidental chemical releases [16]. This wind speed was used in the model, along with the 99th percentile wind speed for the Starlight site, which is approximately 7.2 $\frac{m}{s}$ or 16 mph (see Section 4.1). The wind speeds were defined at an elevation of 10 m above ground level, which is a common height for weather data collection. High wind speeds may partially counteract the buoyant rise of a fire plume, increasing downwind transport. Consistent with EPA guidance, all scenarios were initially evaluated under stability class F conditions to represent worst-case atmospheric stability. However, in accordance with San Diego County requirements, additional analyses were conducted to compare results across stability classes D, E, and F. Specifically, the worst-case concentration scenarios were re-evaluated under each stability class to assess the sensitivity of dispersion to atmospheric conditions. The ambient temperature was modeled as being 77°F or 25°C as required by San Diego County.

Atmospheric stability in the model was characterized using the Obukhov length, following guidance from the FDS User Guide. An Obukhov length of 350 m was used to represent stable conditions (class F), 500 m for slightly stable conditions (class E), and 1,000,000 m for neutral conditions (class D). These values provide a practical representation of atmospheric stability effects on plume dispersion within the modeling framework. The results presented here therefore approximate worst-case conditions based on the combination of wind speed and a range of stability classes. Because the Starlight site is in an area surrounded by farm fields, a closed Davenport-Wieringa roughness length of 0.25 m was used.

The wind speeds used in the models are intended to be worst-case. Therefore, results from other wind speeds are expected to be bounded by the wind speeds used. In addition, evaluating multiple atmospheric stability classes using representative Obukhov lengths provides a means of bounding the influence of atmospheric stability on plume dispersion and captures the range of potential concentration outcomes from stable to neutral conditions.

## 8.2 Results

Model results for combustion product, sulfur dioxide ($SO_2$), and hydrogen fluoride (HF) concentrations were measured at 2 m (6.6 ft) and 5 m (16 ft) above ground level. The 2 m height corresponds to the concentration that people would experience when standing on level ground near an incident, while the 5 m height represents conditions at roughly a second-story elevation. Figures 18 and 19 show the average combustion product gas concentrations at 2 m (6.6 ft) and 5 m (16 ft) above ground level, respectively, at different distances downwind of the unit. Concentrations are reported beginning 2 m (6.6 ft) away from the burning enclosure. In the region immediately downwind of the enclosure, the turbulence is not expected to be predicted within acceptable engineering uncertainty. As the plume evolves downwind and the flow moves away from the shear induced by the flow over the BESS unit, the model becomes more valid, and error is reduced to within acceptable engineering uncertainty. Figures 18 and 19 show that at both 2 m and 5 m combustion product gas concentrations stay low for the fire scenario with a small fire and low wind. For the high wind scenarios, overall combustion product concentrations may be high near the BESS enclosures but drop quickly away from the enclosures. For the large fire low wind scenario, concentrations measured at 2 m exhibit a slight increase at approximately 200 ft, corresponding to a region where the plume briefly bends back toward the ground. Overall, the large fire scenarios result in the highest combustion product concentrations, although the wind speeds have different effects at different elevations. However, since toxic gases are

only a fraction of the total battery vent gas or combustion products, toxic gas concentrations would be a fraction of these values.

Figures 18 and 19 also indicate that atmospheric stability class has a minimal effect on the predicted concentrations. Scenarios evaluated under stability classes D, E, and F, while otherwise identical, produced very similar concentration profiles. This suggests that, for the conditions modeled, plume behavior is relatively insensitive to variations in atmospheric stability within this range.

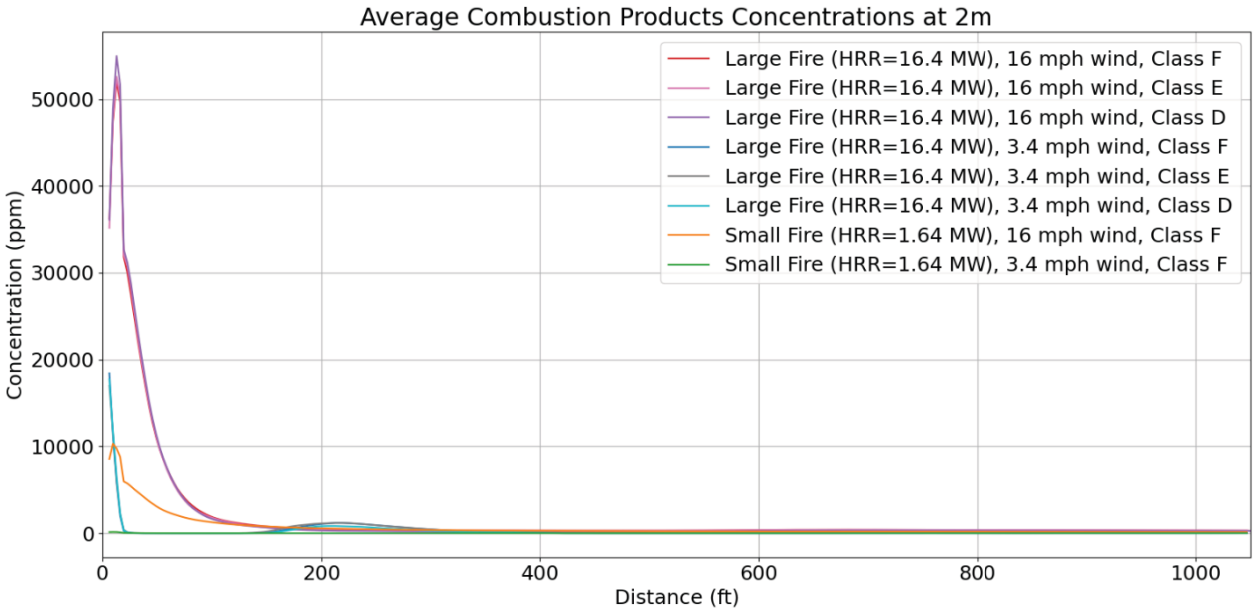


Figure 18: The average battery vent gas or combustion products concentration 2 m (6.6 ft) above ground level versus the downwind distance (starting 2 m from the enclosure) for different model scenarios.

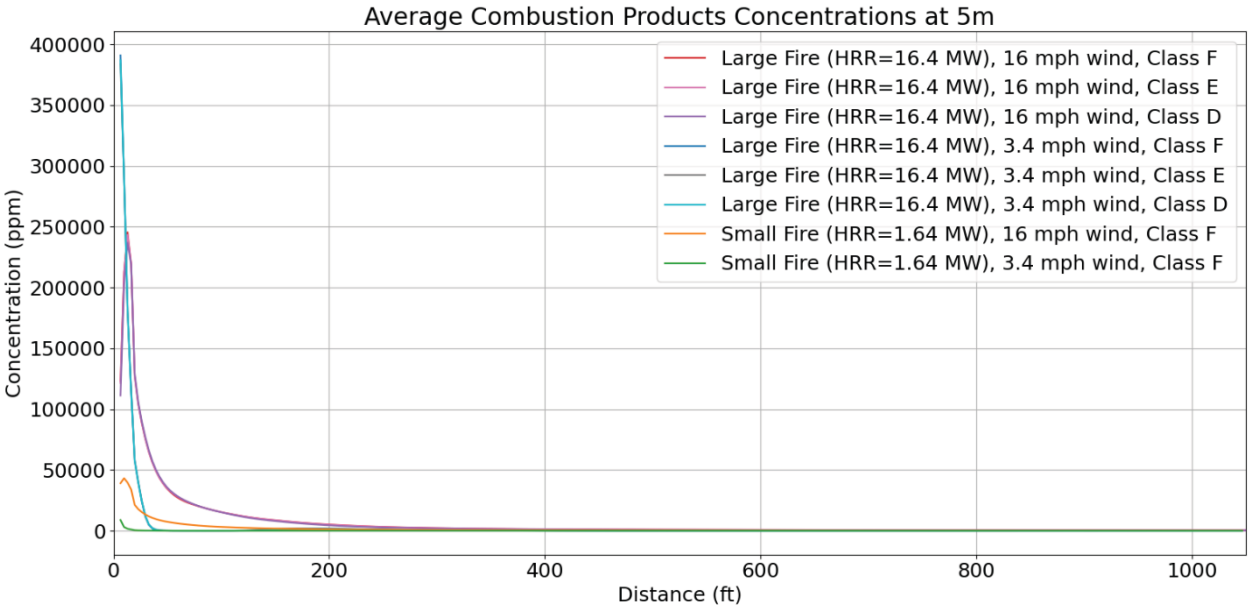


Figure 19: The average battery vent gas or combustion products concentration 5 m (16 ft) above ground level versus the downwind distance (starting 2 m from the enclosure) for different model scenarios.

Buoyancy due to the heat from fire conditions causes the plume to rise away from the ground. In most common wind conditions, where the wind is mild, fire product concentrations are low at ground level as the buoyancy from the fire allows the plume to rise rapidly before being transported downwind. Under conditions of high wind, this buoyant effect may be partially overcome by the higher momentum crosswind resulting in a plume trajectory that is closer to the ground and higher fire product concentrations at the ground level. However, at greater distances downwind, the concentration profiles for the large fire low wind and high wind scenarios at both elevations begin to converge as the fire products at the ground level have been almost completely diluted by mixing. Approximately 200 ft downwind, the large fire low wind concentration profiles are observed to increase slightly and then decrease.

The following figures presented here are for stability class F conditions. As discussed previously, atmospheric stability class was found to have a minimal effect on predicted concentrations, and therefore the stable condition results are considered representative. Figure 20 shows the model with a full unit fire at high wind speeds. This figure shows that the hot combustion products do not rise immediately due to high wind conditions, but they do rise gradually. This scenario was modeled over an extended domain 1500 m (4920 ft) to capture the increased plume transport distance. Additionally, mixing occurs as the combustion products move away from the enclosure. In contrast, Figure 21 shows that under low wind conditions the combustion products rise more steeply due to higher plume buoyancy in relation to wind momentum.

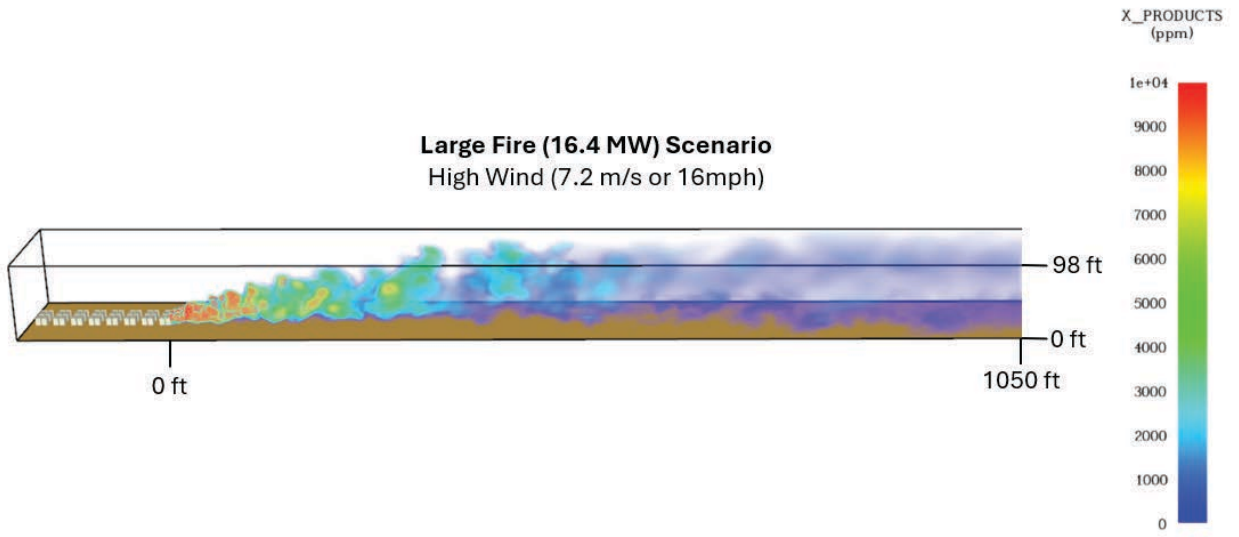


Figure 20: An instantaneous plume model of a full unit fire with high wind and stability class F conditions. X_PRODUCTS is the concentration of combustion products in ppm. The distances shown are measured from the front of the enclosure. For clarity of visualization, the model has been shortened in the horizontal direction to 1,050 ft.

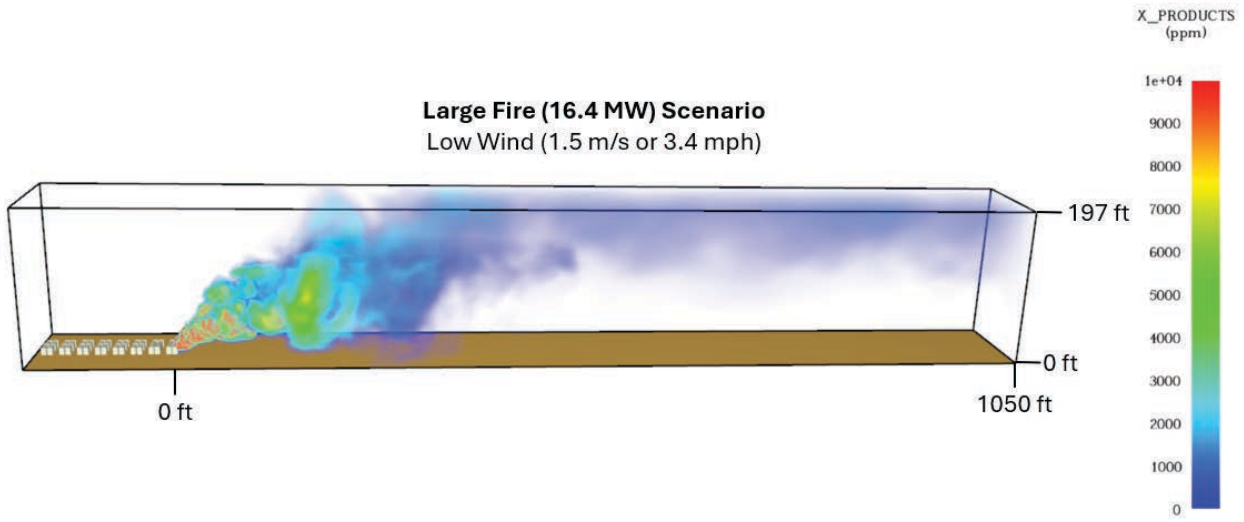


Figure 21: An instantaneous plume model of a full unit fire with low wind and stability class F conditions. In this scenario, combustion products initially rise due to buoyancy. X_PRODUCTS is the concentration of combustion products in ppm. The distances shown are measured from the front of the enclosure.

Figure 22 shows that for a smaller fire with high winds the combustion products stay near ground level. Under low wind conditions, combustion products from a small fire also rise; however, the release rate of combustion products is much smaller than the large fire scenario. The lower release rate and rapid mixing induced by the wind results in a smaller plume and lower ground level concentrations. Figure 23 shows the plume combustion products for small fire low

wind conditions. Similar to the effect on the large fire, the lower wind results in a plume that is not ground-bound and rises higher above the ground level.

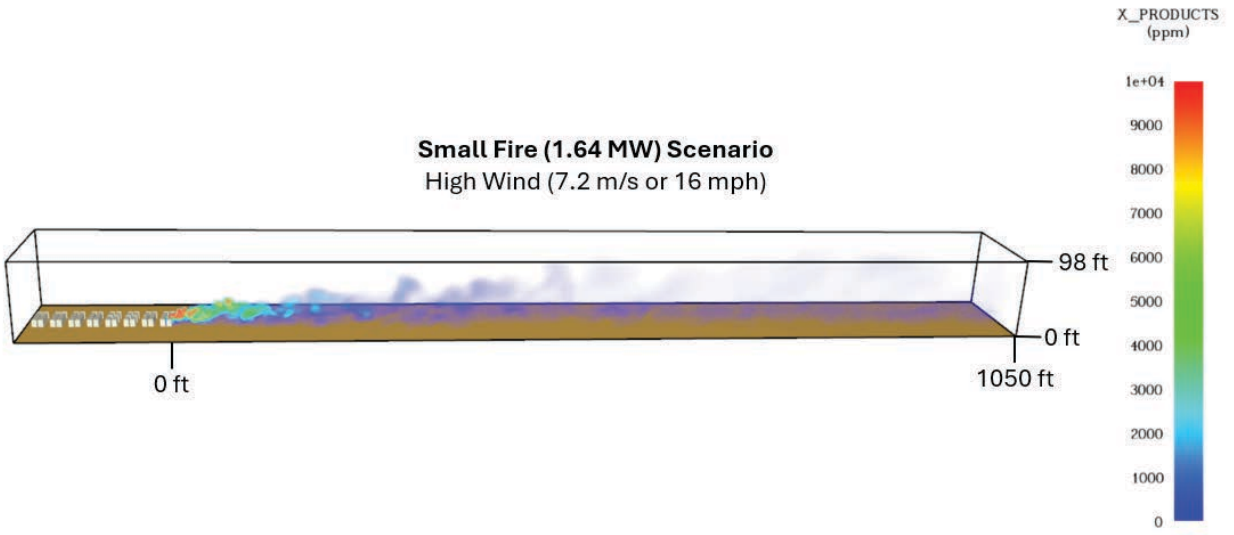


Figure 22: An Instantaneous plume model of a small fire with high wind and stability class F conditions. X_PRODUCTS is the concentration of combustion products in ppm. The distances shown are measured from the front of the enclosure.

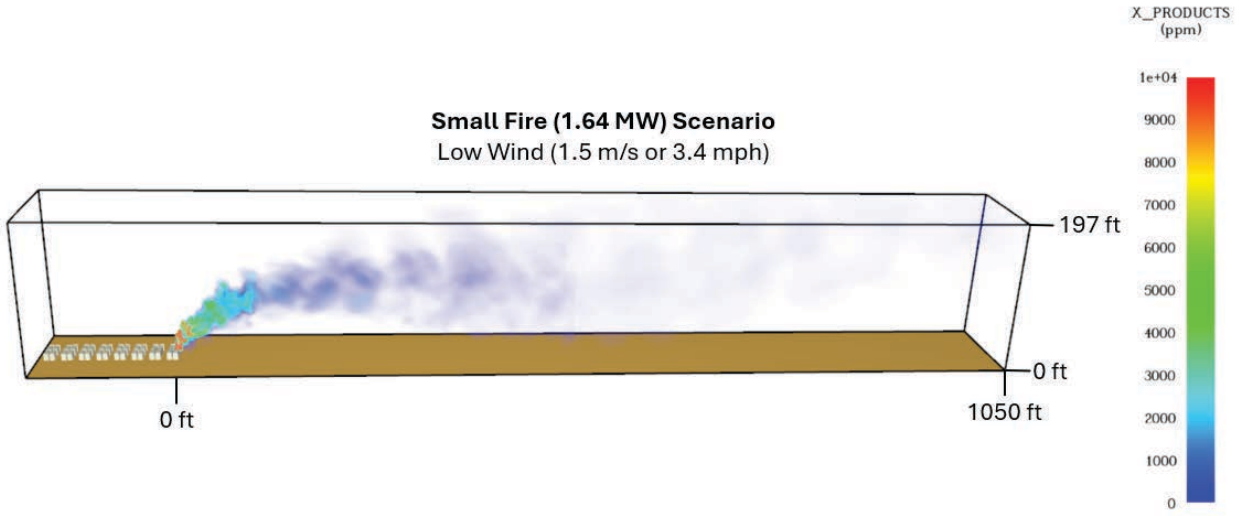


Figure 23: An instantaneous plume model of a small fire with low wind and stability class F conditions. X_PRODUCTS is the concentration of combustion products in ppm. The distances shown are measured from the front of the enclosure.

Although battery vent gases may be made up of multiple toxic gas components, carbon monoxide (CO) is generally the most abundant toxic gas of concern that is regularly reported as part of UL 9540A testing. The UL 9540A cell test report for the Megapack 2 XL listed the carbon monoxide concentration as 10.9%. However, for fire scenarios where the battery vent gases burn, it is unclear what concentration of carbon monoxide may persist through a fire. Because CO is

flammable, the carbon monoxide concentration in burned gas is likely to be much lower than in the battery gas. However, the carbon monoxide concentration is not expected to be zero due to incomplete combustion from the fire, which can vary depending on the burning environment. While a 2% CO yield is commonly assumed in similar analyses, Jensen Hughes, on behalf of San Diego County, recommended a more conservative value of 5% of the combustion products. The average carbon monoxide concentration over the 320 m (1050 ft) model domain for the fire scenarios is shown in Figures 24 and 25, at 2 m and 5 m above ground level, respectively. Measurements begin at a distance of 2 m from the front of the enclosure. For the high wind large fire scenarios, the computational domain was extended to 1500 m (4920 ft) to account for increased plume transport distances. The IDLH (Immediately Dangerous to Life and Health) level for carbon monoxide is 1200 ppm, the AEGL-3 (life-threatening health effects) level for a 30-minute exposure is 600 ppm, and the AEGL-2 (serious health effects) level for a 30-minute exposure is 150 ppm. The EPA does not provide an AEGL-1 (temporary irritation) concentration for carbon monoxide. Model results show that the carbon monoxide concentration may be immediately dangerous to life and health (above the IDLH level) up to approximately 9.7 m (31.7 ft), cause life-threatening effects (exceed the AEGL-3 level) up to approximately 14.7 m (48.2 ft), and cause serious health effects (exceed the AEGL-2 level) up to approximately 25.7 m (84.2 ft) from the burning enclosure. The worst-case distances for 2 m and 5 m elevations are listed in Tables 5 and 6, respectively. 30-minute toxicity levels were chosen as evaluation limits based on a characteristic time for an exposure during an evacuation. This characteristic time is a reasonable upper bound for emergency responders; however, evacuation times may vary depending upon the incident environment.

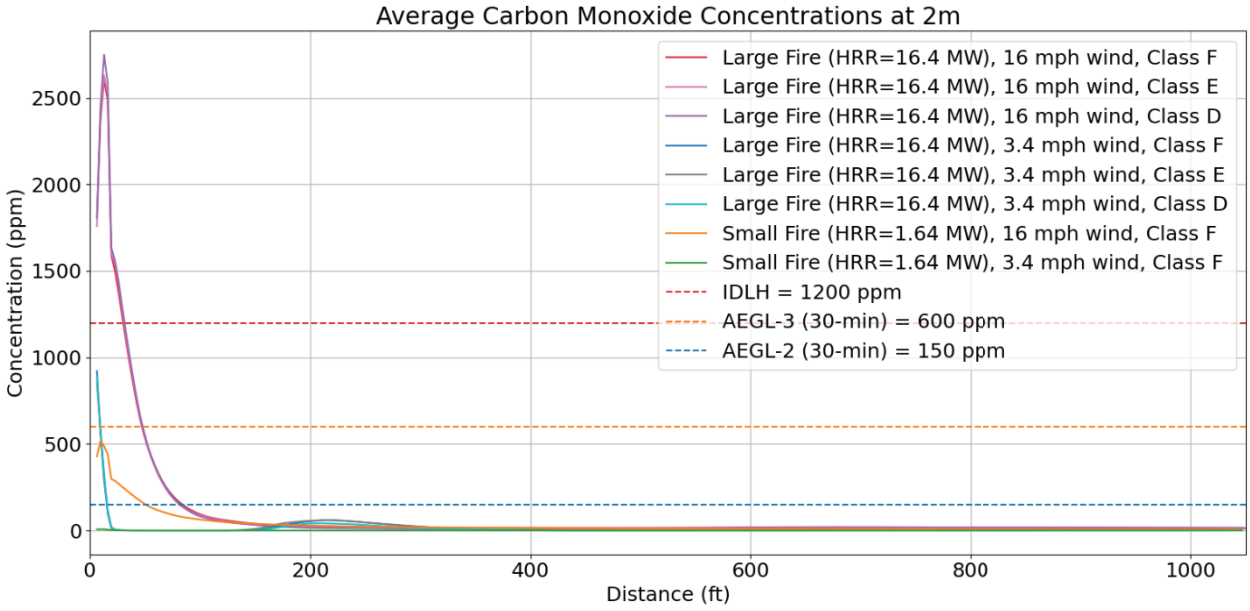


Figure 24: The modeled average carbon monoxide concentrations as a function of distance (starting 2 m from the enclosure) for different combustion product release scenarios at 2 m above ground level.

Table 5: Toxicity levels and worst-case modeled distances for carbon monoxide at 2 m above ground level.

| Toxicity Level for CO | Concentration (ppm) | Modeled Distance at 2 m Elevation | Worst-Case Scenario |
|---|---|---|---|
| **IDLH** | 1200 | 31.7 ft | Large Fire High Wind, Neutral |
| **AEGL-3** | 600 | 48.2 ft | Large Fire High Wind, Neutral |
| **AEGL-2** | 150 | 84.2 ft | Large Fire High Wind, Stable |

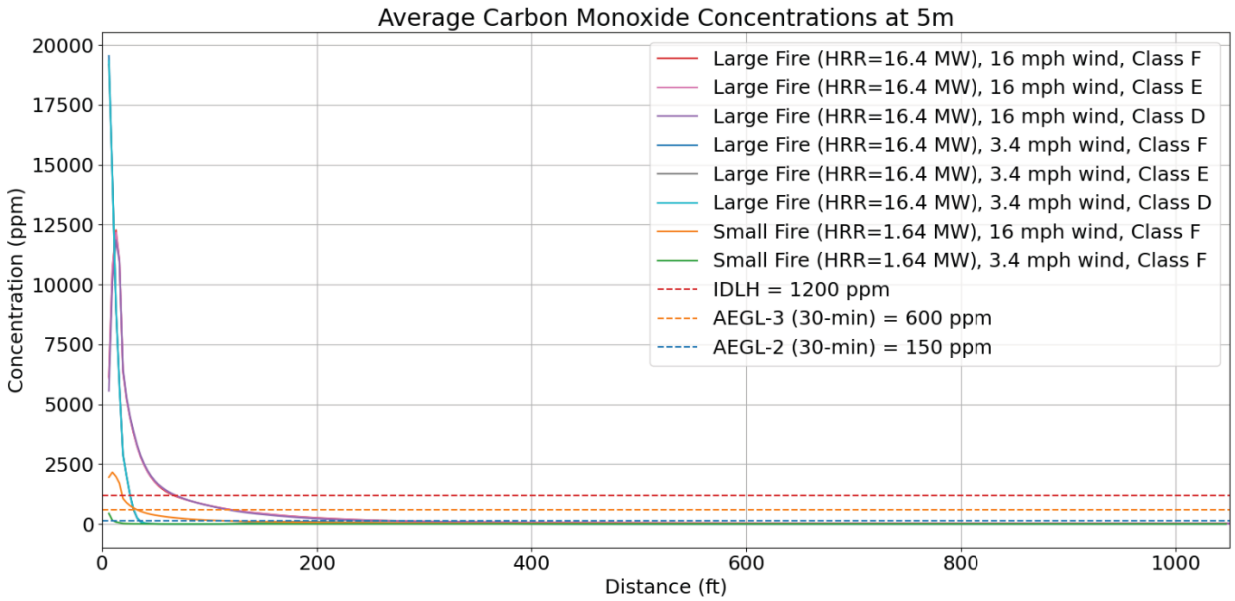


Figure 25: The modeled average carbon monoxide concentrations as a function of distance (starting 2 m from the enclosure) for different combustion product release scenarios at 5 m above ground level.

Table 6: Toxicity levels and worst-case modeled distances for carbon monoxide at 5 m above ground level.

| Toxicity Level for CO | Concentration (ppm) | Modeled Distance at 5 m Elevation | Worst-Case Scenario |
|---|---|---|---|
| **IDLH** | 1200 | 68.6 ft | Large Fire High Wind, Neutral |
| **AEGL-3** | 600 | 120 ft | Large Fire High Wind, Slightly Stable |
| **AEGL-2** | 150 | 259 ft | Large Fire High Wind, Stable |

Hydrogen fluoride (HF) is an acutely toxic gas species whose presence has been reported in some battery failure cases. Due to the high toxicity of hydrogen fluoride at quite low concentrations, it is of growing concern for safety analyses of lithium-ion battery systems. It is well accepted by researchers that a lithium-ion cell can generate HF during thermal runaway. However, HF measurements from large-scale fire tests of BESS are not publicly available. In large-scale BESS fires, hydrogen fluoride production is most likely dominated by the burning of fire-retardant plastics in battery systems rather than by the actual cells. Although the HF generated from lithium-ion cells is not negligible, HF generated from the cells can react with other components such as the module casing or rack structure. Therefore, HF concentrations are likely significantly reduced before being released outside the enclosure. In general, the publicly avail-

able data on hydrogen fluoride in battery failures remains limited, and the reported quantities vary widely. Amounts of hydrogen fluoride between 0 L/Wh and 0.24 L/Wh have been reported [8]. This indicates that HF could represent a significant percentage of the produced gas or not be present in significant amounts. The manner in which this value depends on cell chemistry, state of charge, or other factors is not well understood. Hydrogen fluoride is highly reactive with a range of materials including metals and various organic compounds. It is unclear whether substantial HF concentrations persist at a distance away from larger module, rack, and BESS scales. Hydrogen fluoride can be emitted from combustion of plastic components in the BESS, such as wiring insulation and module or rack enclosure casings. Although these plastics are commonly fire-retarded, fire-retardant plastics can be overwhelmed if the severity of the fire is sufficiently large. Such fire-retardant plastics are commonly found in non-battery applications and may pose similar emission hazards during fire conditions. While some testing laboratories will provide HF data, it is not currently required by UL 9540A or other standards currently in use in the United States. Megapack 2 XL UL 9540A module-level and cell-level test reports indicated that no Hydrogen fluoride was detected, as summarized in the Fisher Engineering report. In a test conducted using the unit-level UL 9540A method, with additional gas sampling performed beyond standard requirements, HF was measured in collected gas samples, with cumulative concentrations of 0.1 ppm and 0.12 ppm over a two-and-a-half-hour period, as summarized in the Fisher Engineering, Inc. report [6].

Sulfur dioxide ($SO_2$) is a toxic gas species that has been reported in some experiments and is attributed to the breakdown of additives in the cell electrolyte during thermal runaway conditions [8]. Like HF, $SO_2$ is not commonly measured, nor required to be measured, during UL 9540A testing. Additionally, little publicly available literature or studies have measured $SO_2$ generation from lithium-ion batteries. $SO_2$ measurements from fire test representative BESS systems are even more limited than HF as no large scale tests conducted have considered $SO_2$. Although testing is limited, $SO_2$ has not been reported by emergency responders during response activities conducted in past BESS fire incidents.

Based upon requests from Jensen Hughes on behalf of San Diego County, sulfur dioxide ($SO_2$) and hydrogen fluoride (HF) were included as additional source terms in the plume analysis for a fire in a single BESS enclosure. The source terms provided by Jensen Hughes were 28 mg/Wh of $SO_2$ and 43.5 mg/Wh of HF. Based on these source terms, the mass percentages of $SO_2$ and HF in the battery gas released in the model are 0.6% and 0.9%, respectively. Furthermore, it was assumed that none of the $SO_2$ or HF reacted away. The provided source terms were included in the model, as requested, although the source of sulfur is unclear and data for HF is based on cell tests rather than full enclosure tests. Because HF is highly reactive, it is likely to react before leaving the enclosure or as the plume disperses. $SO_2$ is also highly reactive with metals and other plume components such as water vapor and oxygen. Assuming that the HF and $SO_2$ generated by the lithium-ion cells do not react with other materials in the BESS enclosure or downstream in the plume likely results in overestimates of HF and $SO_2$ concentrations at the ground level from the plume model.

Unlike the other combustion products, which are assumed to be lumped, both $SO_2$ and HF are modeled as separate species, where species transport equations are individually solved. Modeling $SO_2$ and HF as un-lumped species allows for simulation of stratification of denser-than-air species, if any occurs. The IDLH and AEGL thresholds for $SO_2$ and HF can be found in Section 3.2. Figures 26-27 and 29-30 present the concentration results for $SO_2$ and HF, respectively. Additionally, Tables 7 through 10 summarize the toxicity thresholds and modeled distances for $SO_2$ and HF at both 2 and 5 m of elevation. Figures 28 and 31 show instantaneous views of the $SO_2$ and HF plumes for the large fire high wind, stable scenario. Notably, the upper bounds of the concentration scales in both of these figures are a factor of 10 lower than those used in the plume figures shown earlier in the report. The reduced scales improve visibility of the plume structure at lower concentrations. The corresponding combustion product plume is shown in Figure 20. Although $SO_2$ is denser than air, it is not observed to settle or fall out of the plume.

Stratification of $SO_2$ to the ground level is not expected because the battery gases are well mixed when they are released from the enclosure. As the battery gases travel downwind, convection from the turbulent boundary layer is more dominant than diffusion driven by density differences between $SO_2$ and air. The $SO_2$ remains well-mixed and remains lofted with the other plume products throughout the downstream domain.

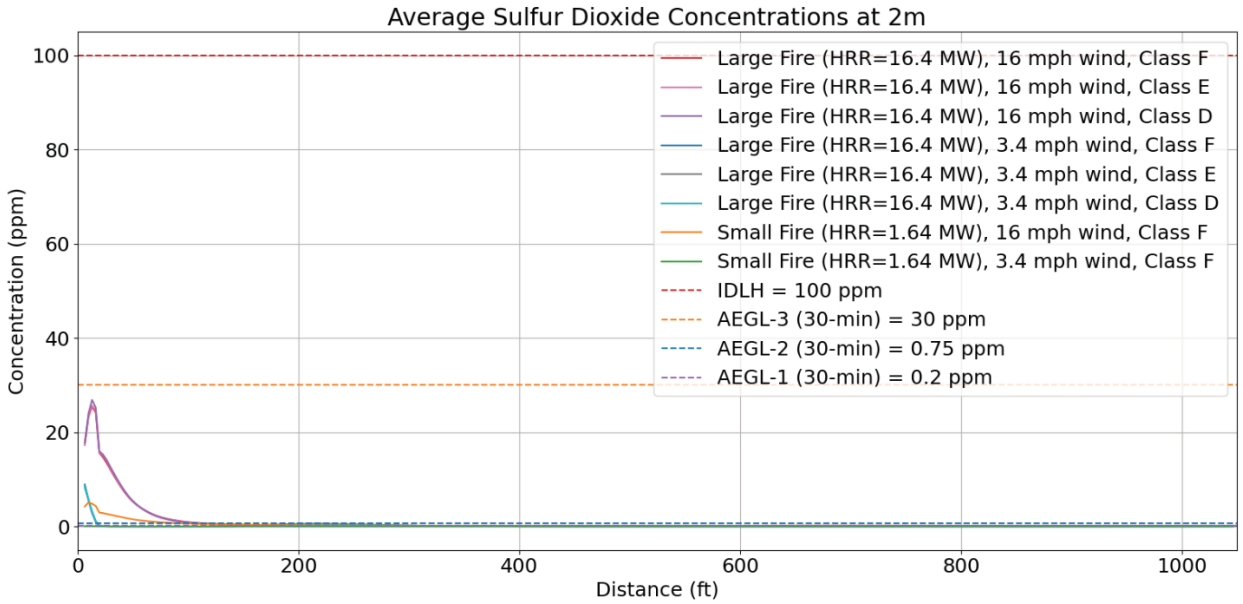


Figure 26: The modeled average sulfur dioxide concentrations as a function of distance (starting 2 m from the enclosure) for different combustion product release scenarios at 2 m above ground level.

Table 7: Toxicity levels and worst-case modeled distances for sulfur dioxide at 2 m above groud level.

| Toxicity Level for SO | Concentration (ppm) | Modeled Distance at 2 m Elevation | Worst-Case Scenario |
|---|---|---|---|
| **IDLH** | 100 | **N/A** | **N/A** |
| **AEGL-3** | 30 | **N/A** | **N/A** |
| **AEGL-2** | 0.75 | 109 ft | Large Fire High Wind, Stable |
| **AEGL-1** | 0.2 | 305 ft | Large Fire Low Wind, Slightly Stable |

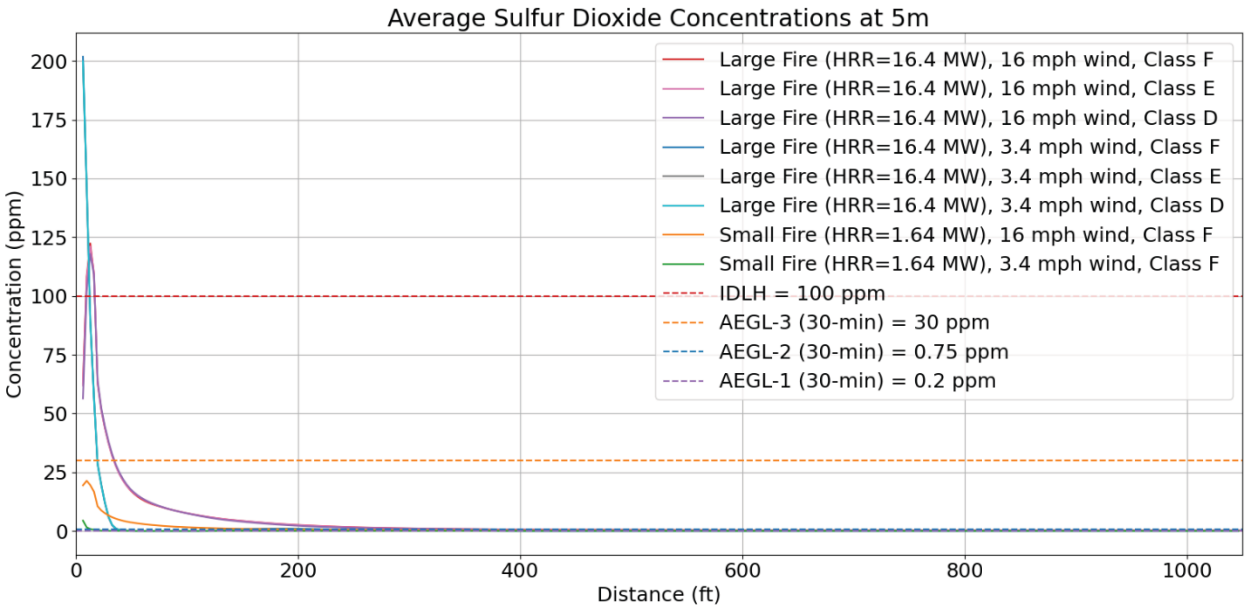


Figure 27: The modeled average sulfur dioxide concentrations as a function of distance (starting 2 m from the enclosure) for different combustion product release scenarios at 5 m above ground level.

Table 8: Toxicity levels and worst-case modeled distances for sulfur dioxide at 5 m above ground level.

| Toxicity Level for SO | Concentration (ppm) | Modeled Distance at 5 m Elevation | Worst-Case Scenario |
|---|---|---|---|
| **IDLH** | 100 | 17.1 ft | Large Fire High Wind, Slightly Stable |
| **AEGL-3** | 30 | 34.8 ft | Large Fire High Wind, Neutral |
| **AEGL-2** | 0.75 | 366 ft | Large Fire High Wind, Slightly Stable |
| **AEGL-1** | 0.2 | 953 ft | Large Fire Low Wind, Stable |


Figure 28: An instantaneous view of the $SO_2$ in the plume assuming a source term of 28 mg/Wh of $SO_2$ for the large fire high wind, stable scenario. Note that the upper bound of this scale is a factor of 10 lower than in Figure 20.

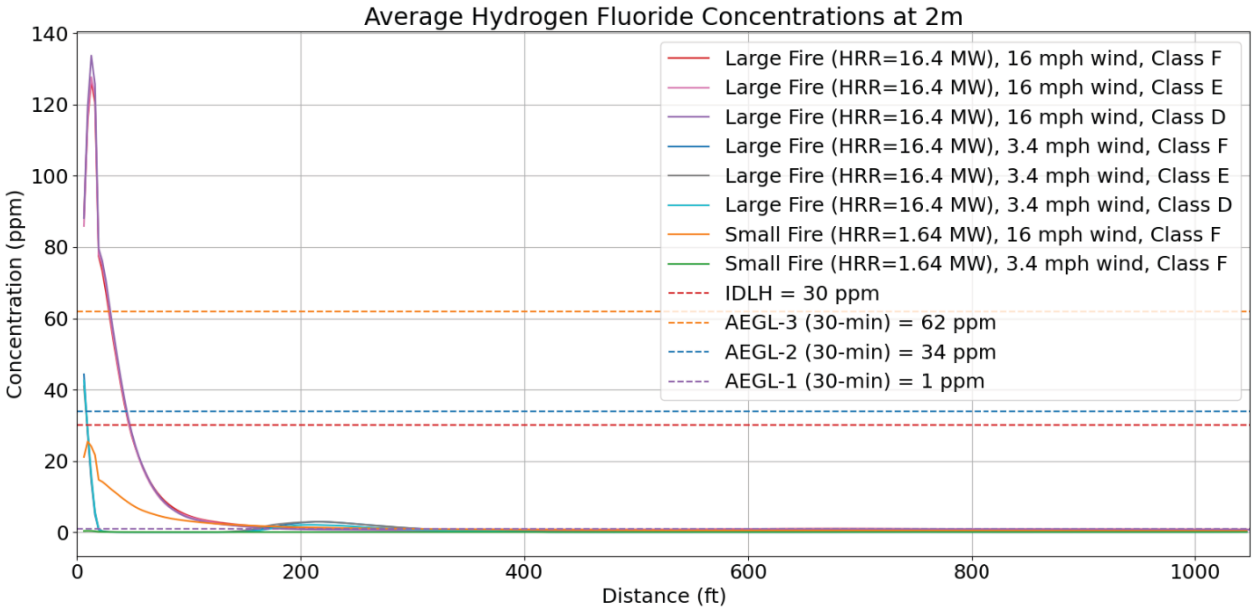


Figure 29: The modeled average hydrogen fluoride concentrations as a function of distance (starting 2 m from the enclosure) for different combustion product release scenarios at 2 m above ground level.

Table 9: Toxicity levels and worst-case modeled distances for hydrogen fluoride at 2 m above ground level.

| Toxicity Level for HF | Concentration (ppm) | Modeled Distance at 2 m Elevation | Worst-Case Scenario |
|---|---|---|---|
| **IDLH** | 30 | 47.7 ft | Large Fire High Wind, Neutral |
| **AEGL-3** | 62 | 30.2 ft | Large Fire High Wind, Neutral |
| **AEGL-2** | 34 | 44.9 ft | Large Fire High Wind, Neutral |
| **AEGL-1** | 1 | 304 ft | Large Fire Low Wind, Slightly Stable |

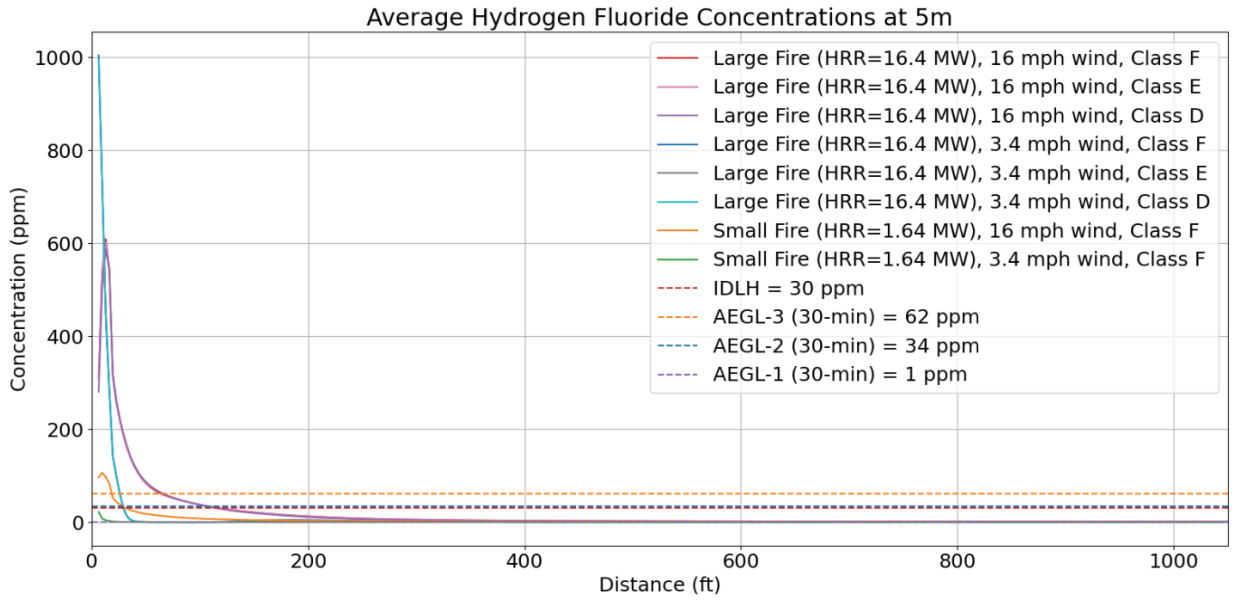


Figure 30: The modeled average hydrogen fluoride concentrations as a function of distance (starting 2 m from the enclosure) for different combustion product release scenarios at 5 m above ground level.

Table 10: Toxicity levels and worst-case modeled distances for hydrogen fluoride at 5 m above ground level.

| Toxicity Level for HF | Concentration (ppm) | Modeled Distance at 5 m Elevation | Worst-Case Scenario |
|---|---|---|---|
| **IDLH** | 30 | 118 ft | Large Fire High Wind, Stable |
| **AEGL-3** | 62 | 65.5 ft | Large Fire High Wind, Neutral |
| **AEGL-2** | 34 | 108 ft | Large Fire High Wind, Stable |
| **AEGL-1** | 1 | 948 ft | Large Fire High Wind, Stable |


Figure 31: An instantaneous view of the HF in the plume assuming a source term of 43.5 mg/Wh of HF for the large fire high wind, stable scenario. Note that the upper bound of this scale is a factor of 10 lower than in Figure 20.

Typically, hydrocarbons such as benzene and toluene are the only toxic gas concentrations other than carbon monoxide that are measured as part of the UL 9540A testing process. These do not present significant toxicity hazards compared to carbon monoxide, sulfur dioxide, and hydrogen fluoride, as their concentrations in battery gas are usually orders of magnitude less while having generally higher AEGL concentrations than CO, $SO_2$, and HF. For the Contemporary Amperex Technology Co., Ltd. (CATL) cells, the benzene and toluene concentrations are 0.002% and 0.002%, respectively.

# 9 Conclusion

Of the measured toxic gas species for which test data is available, carbon monoxide is of primary concern due to its comparatively high concentrations and toxicity. Carbon monoxide has an IDLH (immediately dangerous to life and health) level of 1200 ppm, an AEGL-3 (life-threatening health effects) level for a 30-minute exposure of 600 ppm, and an AEGL-2 (serious health effects) level for a 30-minute exposure of 150 ppm. No AEGL-1 level is provided for CO. Carbon monoxide may constitute up to 10.9% of the unburned battery vent gas based upon the publically available Fisher Engineering report summary of the UL 9540A cell-level report. Carbon monoxide concentrations 2 m (6.6 ft) from ground level were calculated using modeled fire product concentrations and typical carbon monoxide levels present during lithium-ion battery fires. The modeled average carbon monoxide concentrations may be immediately dangerous to life and health (exceed the IDLH level) up to 9.7 m (31.7 ft), cause life-threatening health effects (exceed the AEGL-3 level) up to 14.7 m (48.2 ft), and cause serious health effects (exceed the AEGL-2 level) up to approximately 25.7 m (84.2 ft) from the unit in a large fire scenario with high winds. The modeled high wind speed of 7.2 $\frac{m}{s}$ (16 mph) is the 99th percentile wind speed at the Starlight site. These distances are based on concentrations evaluated beginning 2 m (6.6 ft) from the enclosure. A burning enclosure should not be approached during an incident. Toxic levels were reached in scenarios with low wind or smaller fire conditions; however, these did not represent worst-case conditions and resulted in shorter downwind impact distances than those listed above.

Hydrogen fluoride was not measured during the UL 9540A unit-level, module-level, or cell-level testing for the Megapack 2 XL system. However, during the additional extended UL 9540A unit-level testing, hydrogen fluoride was detected in collected gas samples. The modeled results at 2 m above ground level indicated hydrogen fluoride concentrations below the AEGL-1 threshold at 304 ft. As the BESS system has not yet been finalized in this project, the magnitude of hydrogen fluoride risk remains uncertain. If quantification of HF levels are desired, it is recommended that additional fire testing beyond the scope of the UL 9540A testing be performed in order to quantify what levels of hydrogen fluoride may exist for the finalized BESS system. Sulfur dioxide was also not measured during the UL 9540A module-level, cell-level or large scale fire testing for the Megapack 2 XL system. However, modeled results at 2 m above ground level based on source terms provide by Jensen Hughes indicated sulfur dioxide concentrations below AEGL-1 thresholds at 305 ft. Neither HF nor $SO_2$ has been reported by emergency responders during past BESS fire incidents. Other measured toxic gases make up only trace amounts of the battery vent gas. Hydrocarbon release quantities are too small to exceed IDLH or AEGL levels at any distance from the unit.

Provided planning documents [1] and publicly available maps indicate that the Starlight site is in a relatively isolated location. The nearest exposure is approximately 1235 ft away from the nearest BESS enclosure. Other single homes are scattered around the site. An elementary school is located approximately 1.15 miles northwest of the nearest BESS enclosure (see Figure 2). Based on the model results and the prevailing wind direction at the site, it is unlikely that nearby homes will experience toxic levels of carbon monoxide in the event of a single BESS unit experiencing a failure. Even assuming conservative HF and $SO_2$ source terms, it is unlikely that nearby homes or buildings will experience toxic levels of HF and $SO_2$ in the event of a single BESS unit experiencing a failure.

Given the potential risk of toxicity hazards during failure scenarios of the BESS, appropriate emergency response protocols should be considered and developed in collaboration with local emergency personnel. During an incident, site conditions may change and should be monitored throughout the incident. Changes in conditions may require appropriate adjustment to response measures. Additional discussion of emergency response protocols may be provided in a separate emergency response guideline document. Figure 32 shows the areas that could have toxic carbon monoxide gas concentrations exceeding the IDLH level (immediately dangerous to life and health), AEGL-3 level (life-threatening health effects), and the AEGL-2 level (serious health effects) based on the worst-case modeled scenarios for high winds at the Starlight project site. These distances were measured from the outermost BESS enclosures. Note that this figure does not consider possible sulfur dioxide or hydrogen fluoride concentrations.

Separate buffer maps were not developed for sulfur dioxide or hydrogen fluoride. Sulfur dioxide was not included due to the lack of evidence indicating that it would be generated in meaningful quantities for the evaluated scenarios, and it is a highly reactive species. Hydrogen fluoride was also not mapped because it is a highly reactive species. Representing both HF and $SO_2$ as passive, inert dispersing gases would not accurately capture their behavior and could lead to misleading spatial predictions. However, estimated distances to AEGL-1 toxicity limits based on these assumptions are not expected reach nearby homes or buildings.

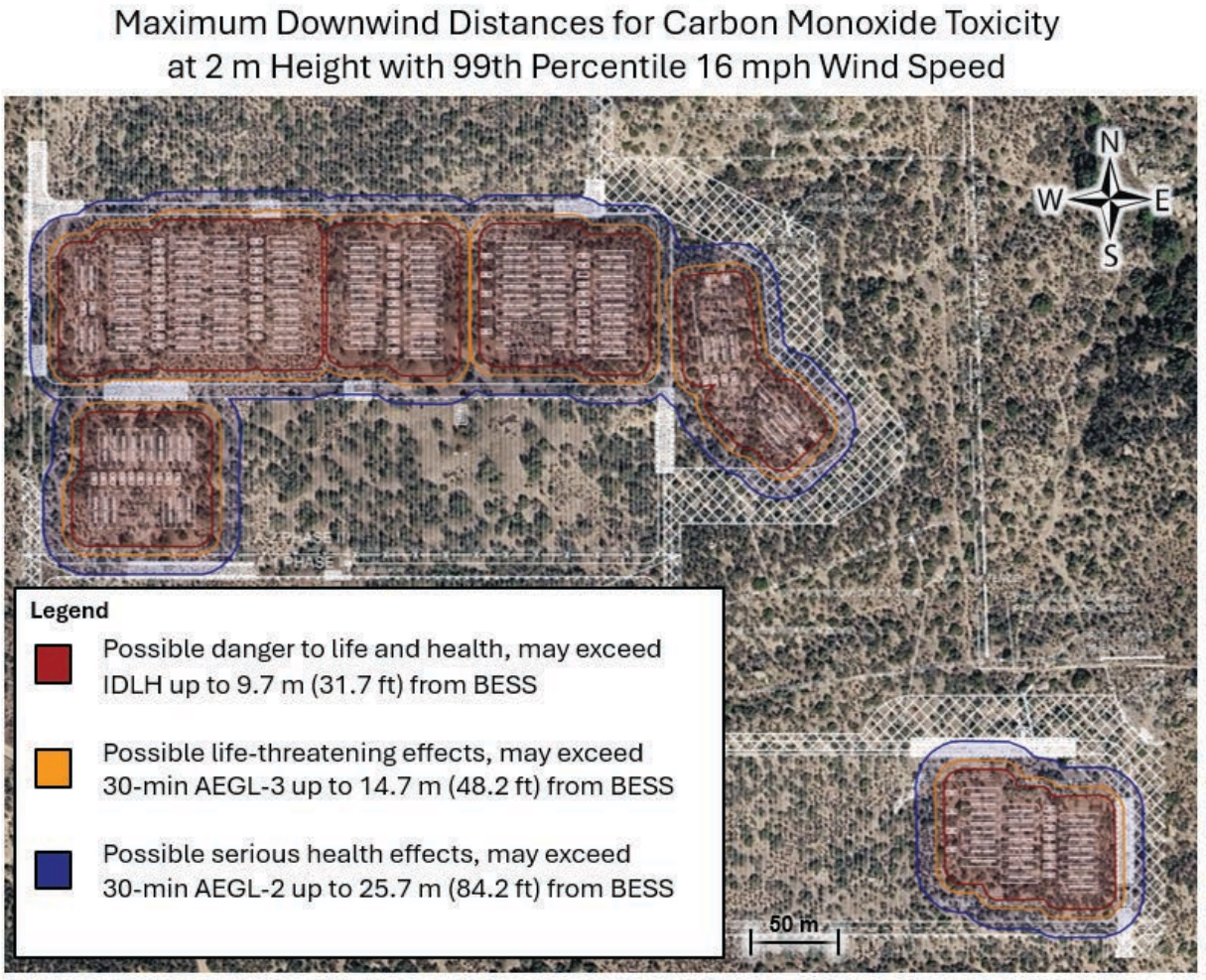


Figure 32: Satellite imagery of the immediate site surroundings with overlaid areas indicating possible IDLH, AEGL-3, and AEGL-2 levels of toxic gases under steady 7.2 $\frac{m}{s}$ (16 mph) winds, corresponding to the 99th percentile wind speed for the Starlight site, with concentrations evaluated at a 2 m receptor height. Note that these buffers do not account for possible sulfur dioxide or hydrogen fluoride concentrations. This image was produced using Open Street Map and Google Maps.

The buffers in Figure 32 show the maximum modeled distances for critical carbon monoxide concentrations in all possible wind conditions. In reality, the wind will only come from one direction at a time, so a plume resulting from BESS failure will travel predominantly in one direction. Figure 33 shows a modeled plume for a high wind coming from the east.

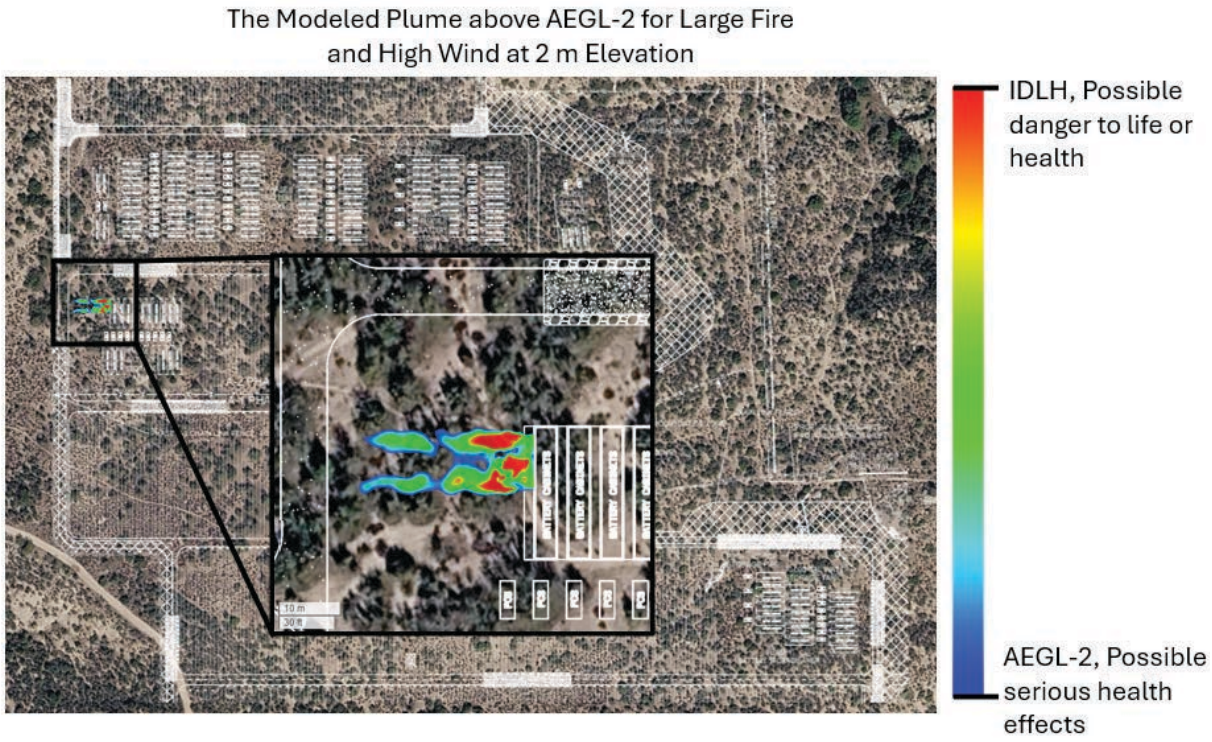


Figure 33: Satellite imagery of the immediate site surroundings with an overlaid plume that was modeled with 16 mph wind from the east. Note that this plume does not consider possible sulfur dioxide or hydrogen fluoride levels. This image was produced using Open Street Map and Google Maps.

The analysis in this report assumes that only one battery unit fails or burns at a time. There may be several conditions that could lead to worse consequences than those predicted by this model. These conditions include, but are not limited to, thermal runaway propagation exceeding the measured release rate and involvement of multiple units. However, based on the analysis presented in *Preliminary Fire Risk Assessment and Heat Flux Analysis* document, these scenarios are unlikely [7].

# 10 Limitations

- The study presented in this report is intended for use by client to assist with their decision making related to toxicity risks due to plume transport and evolution from Lithium-ion Battery Energy Storage Systems (BESS). This study specifically does not address other energy storage designs, feasibility of other toxic gas mitigation methods, or compliance to local codes and standards. The scope of the analysis was strictly limited to collection of data relevant to scope.
- The scope of services performed may not adequately address the needs of other users of this report, and any re-use of this report is at the sole risk of the user. This study is based on observations and information available at the time of the analysis. No guarantee or warranty as to future life or performance of any reviewed condition is expressed or implied.
- In the analysis, we have relied on documentation, including but not limited to facility design, BESS design, and other siting documents provided by the client. We cannot

verify the correctness of this data and rely on the client for their accuracy. Although we have exercised usual and customary care in the conduct of this analysis, the responsibility for the design and manufacture of the product remains fully with the client.

- The methodology forming the basis of the results presented in this report is based on mathematical modeling of physical systems and data from third parties. Given the nature of these evaluations, significant uncertainties are associated with the various computations. These uncertainties are inherent in the methodology and subsequently in the generated results. Furthermore, the assumptions adopted do not constitute the exclusive set of reasonable assumptions, and use of a different set of assumptions or methodology could produce materially different results.

# References

[1] *Starlight Site Plan BESS*. SWCA, December 2024, no. 53792.

[2] K. Butts, *Starlight Solar County of San Diego, CA Major Use Permit*. Michael Baker International, March 2024, no. PDS2022-MUP-22-010.

[3] *Megapack 2XL Datasheet*. Tesla, Inc., February 2023, no. Rev. 1.5.1. [Online]. Available: https://portal.ct.gov/-/media/csc/3_petitions-medialibrary/petitions_medialibrary/mediapetitionnos1601-1700/pe1607/petitionersubmissions/supplement-attachment-a---megapack_2_xl_datasheet.pdf

[4] *Megapack 2 XL Safety Overview*. Tesla, Inc., September 2022, no. Rev 1.0. [Online]. Available: https://os-data-2.s3-ap-southeast-2.amazonaws.com/hsc/bundle457/attachment_6_-_megapack_2_xl_safety_overview_3.pdf

[5] *Tesla Pre-PO Engineering Review Requirements*. Energy Toolbase, January 2024, no. Revision 2.7. [Online]. Available: https://help.energytoolbase.com/hc/en-us/articles/34180789868948-Tesla-Pre-PO-Engineering-Review-Requirements#:~:text=Depending%20on%20the%20project%2C%20please,prevent%20resonance%20in%20the%20system.&text=There%20is%20a%20link%20to,possible%20with%20your%20project%20information.&text=This%20checklist%20(linked%20at%20bottom,familiarize%20yourself%20with%20this%20checklist.

[6] *Fire Protection Engineering Analysis*. Fisher Engineering, Inc., January 2023, no. 22035. [Online]. Available: https://www.tarrytownny.gov/sites/g/files/vyhlif1306/f/uploads/megapack_2_xl_fpe_report_final.pdf

[7] *Battery Energy Storage System Preliminary Fire Risk Assessment and Heat Flux Analysis*. Hiller, July 2025, no. Revision 2.

[8] O. Willstrand, R. Bisschop, P. Blomqvist, A. Temple, and J. Anderson, "Toxic Gases from Fire in Electric Vehicles," *RISE*, p. 240, 2020.

[9] 3M, "3M Novec-1230 Fire Protection Fluid Technical Data," Feb. 2022. [Online]. Available: https://multimedia.3m.com/mws/media/1246880/3m-novec-1230-fire-protection-fluid.pdf

[10] D. A. Purser, "Combustion Toxicity," in *SFPE Handbook of Fire Protection Engineering*, M. J. Hurley, D. Gottuk, J. R. Hall, K. Harada, E. Kuligowski, M. Puchovsky, J. Torero, J. M. Watts, and C. Wieczorek, Eds. New York, NY: Springer, 2016, pp. 2207–2307. [Online]. Available: https://doi.org/10.1007/978-1-4939-2565-0_62

[11] "29 CFR 1910.120 – Hazardous waste operations and emergency response." [Online]. Available: https://www.ecfr.gov/current/title-29/subtitle-B/chapter-XVII/part-1910/subpart-H/section-1910.120

[12] "Immediately Dangerous to Life or Health | NIOSH | CDC," Jul. 2020. [Online]. Available: https://www.cdc.gov/niosh/idlh/default.html

[13] O. US EPA, "Acute Exposure Guideline Levels for Airborne Chemicals," Jul. 2022. [Online]. Available: https://www.epa.gov/aegl

[14] "Wind roses," March 2026. [Online]. Available: https://mesonet.agron.iastate.edu/sites/windrose.phtml?station=BVDC1&network=CA_DCP

[15] *Specification Sheet GridSolv Quantum*. Wartsila Energy Storage and Optimisation, September 2023.

[16] U. EPA, “Risk Management Program Guidance for Offsite Consequence Analysis,” U.S. Environmental Protection Agency, Tech. Rep. EPA 550-B-99-009, Mar. 2009. [Online]. Available: https://www.epa.gov/sites/default/files/2013-11/documents/oca-chps.pdf

[17] e. a. Sobianowska-Turek, *The Necessity of Recycling of Waste Li-Ion Batteries Used in Electric Vehicles as Objects Posing a Threat to Human Health and the Environment*. Recycling, no. recycling6020035.

[18] B. Ditch and D. Zeng, *Development of Sprinkler Protection Guidance for Lithium Ion Based Energy Storage Systems*. FM Global, no. PROJECT ID RW000029.

[19] *SFPE Handbook of Fire Protection Engineering*. Springer, no. Fifth Edition.

# 11 Appendix

## 11.1 Heat Release Rate Calculation

The heat release rate (HRR) for a large fire scenario was calculated assuming that all cells fully burn. The casing of the modules was assumed to be metal based on pictures in the Fisher Engineering Report. Other flammable components in the enclosure, such as wire insulation, etc., were not considered. The timing for the calculation was taken from the timeline of the destructive unit-level test [6]. The HRR was assumed to have a trapezoidal shape with a ramp up time of 6556 s and a ramp down time of 14 640 s. The peak burn time was taken to be 5400 s based on test data. Estimations for cell composition, material heats of combustion, and other material properties were taken from the literature and other reputable sources [17, 18, 19].

### 1 Heat Release Rate

$$w_{electrolyte} = 0.149$$

$$w_{plastic} = 0.044$$

$$m_{cell} = 2.991 \text{ kilogram}$$

$$m_{electrolyte} = w_{electrolyte} \cdot m_{cell} = 0.149 \cdot 2.991 \text{ kilogram} = 0.446 \text{ kilogram}$$

$$m_{plastic} = w_{plastic} \cdot m_{cell} = 0.044 \cdot 2.991 \text{ kilogram} = 0.132 \text{ kilogram}$$

$$\text{Hc}_{electrolyte} = 28 \cdot \frac{\text{MJ}}{\text{kg}} = 28 \cdot \frac{1.000 \text{ megajoule}}{1.000 \text{ kilogram}} = 28.000 \frac{\text{megajoule}}{\text{kilogram}}$$

$$\text{Hc}_{plastic} = 38 \cdot \frac{\text{MJ}}{\text{kg}} = 38 \cdot \frac{1.000 \text{ megajoule}}{1.000 \text{ kilogram}} = 38.000 \frac{\text{megajoule}}{\text{kilogram}}$$

$$\rho_{polypropylene} = 960 \cdot \frac{\text{kg}}{(m)^3} = 960 \cdot \frac{1.000 \text{ kilogram}}{(1.000 \text{ meter})^3} = 960.000 \frac{\text{kilogram}}{\text{meter}^3}$$

$$N_{modules} = 24$$

$$\text{Ncells}_{module} = 336$$

$$\text{Ncells}_{enclosure} = N_{modules} \cdot \text{Ncells}_{module} = 24 \cdot 336 = 8064$$

$$\begin{aligned} E_{cells} &= \text{Ncells}_{enclosure} \cdot \left(m_{electrolyte} \cdot \text{Hc}_{electrolyte} + m_{plastic} \cdot \text{Hc}_{plastic}\right) \\ &= 8064 \cdot \left(0.446 \text{ kilogram} \cdot 28.000 \frac{\text{megajoule}}{\text{kilogram}} + 0.132 \text{ kilogram} \cdot 38.000 \frac{\text{megajoule}}{\text{kilogram}}\right) \\ &= 140953.914 \text{ megajoule} \end{aligned}$$

$$\text{Peak}_{BurnTime} = 5400.000 \text{ second (From LSFT)}$$

$$\text{Total}_{BurnTime} = 26596.000 \text{ second (From LSFT)}$$

$$\text{Total}_{Duration} = \text{Peak}_{BurnTime} + \text{Total}_{BurnTime} = 5400.000 \text{ second} + 26596.000 \text{ second} = 31996.000 \text{ second}$$

$$\text{HRR} = \frac{E_{cells} \cdot 2}{\text{Total}_{Duration}} = \frac{140953.914 \text{ megajoule} \cdot 2}{31996.000 \text{ second}} = 8.811 \frac{\text{megajoule}}{\text{second}}$$

# 12 Revisions

Table 11: Document revision history.

| Revision | Date | Description |
|---|---|---|
| 0.1 | April 21 2026 | Initial draft version submitted to client for review. |